Published for SISSA by Springer

Received: *October 11, 2024*
Revised: *January 23, 2025*
Accepted: *March 3, 2025*
Published: *April 15, 2025*

Search for heavy long-lived charged particles with large ionization energy loss in proton-proton collisions at $\sqrt{s} = 13$ TeV

The CMS collaboration

E-mail: cms-publication-committee-chair@cern.ch

Abstract: A search for heavy, long-lived, charged particles with large ionization energy loss within the silicon tracker of the CMS experiment is presented. A data set of proton-proton collisions at a center of mass energy at $\sqrt{s} = 13$ TeV, collected in 2017 and 2018 at the CERN LHC, corresponding to an integrated luminosity of 101 fb^{-1}, is used in this analysis. Two different approaches for the search are taken. A new method exploits the independence of the silicon pixel and strips measurements, while the second method improves on previous techniques using ionization to determine a mass selection. No significant excess of events above the background expectation is observed. The results are interpreted in the context of the pair production of supersymmetric particles, namely gluinos, top squarks, and tau sleptons, and of the Drell-Yan pair production of fourth generation (τ') leptons with an electric charge equal to or twice the absolute value of the electron charge (e). An interpretation of a Z' boson decaying to two τ' leptons with an electric charge equal to $2e$ is presented for the first time. The 95% confidence upper limits on the production cross section are extracted for each of these hypothetical particles.

Keywords: Beyond Standard Model, Hadron-Hadron Scattering, Lifetime, Tau Physics

ArXiv ePrint: 2410.09164

https://doi.org/10.1007/JHEP04(2025)109

JHEP04(2025)109

Contents

1 Introduction

Many extensions of the standard model (SM) include heavy, long-lived, charged particles that could be produced at the CERN LHC with speeds significantly less than the speed of light [1–3], and/or electric charge Q not equal to $\pm 1e$ [4–9], with e being the absolute value of the electron charge. If particles predicted by these extensions beyond the SM (BSM) are produced at the LHC and they have lifetimes greater than $\mathcal{O}(\,\mathrm{ns})$, they could travel far in the CMS detector before decaying. Large lifetimes are the consequence of small widths and, indeed, BSM particles can have small total decay widths as the result of small couplings to their decay products, suppressed phase space, or large mediator mass scales. If such a particle carries electric charge, it can be generically referred to as a heavy stable charged particle (HSCP), even though it may actually be metastable.

For HSCPs with mass greater than about 100 GeV, a significant fraction of BSM particles produced at the LHC will have a relative velocity, $\beta \equiv v/c$, significantly smaller than 1. Such particles can be separated from ultra-relativistic lower-mass SM particles because of their higher rate of ionization energy loss ($\mathrm{d}E/\mathrm{d}x$). This paper describes a search for HSCPs using measurements of $\mathrm{d}E/\mathrm{d}x$ in the CMS pixel and silicon strip detectors.

The dependence of $\mathrm{d}E/\mathrm{d}x$ on particle momentum is described by the Bethe-Bloch formula [10]. Searching for candidates at large momentum with larger $\mathrm{d}E/\mathrm{d}x$ deposits gives

JHEP04(2025)109

sensitivity to slow, massive particles with $|Q| = 1e$ and particles with $|Q| > 1e$, as the SM particles have nearly uniform collected charge per unit of path length at the minimum ionizing particle (MIP) level (with a mean of $\approx$3.9 MeV/cm in silicon).

Previous collider searches for HSCPs were performed at the CERN LEP collider [11–14], DESY HERA collider [15], the Fermilab Tevatron [16–19], and the LHC [20–34], each placed upper cross section limits on various HSCP models. The most recent previous CMS results based on data recorded in 2015 [33] place lower limits at 95% confidence level (CL) on the mass of gluinos, top squarks, and pair-produced tau sleptons. An analysis [34] based on tracker $\mathrm{d}E/\mathrm{d}x$ information only, performed by the ATLAS Collaboration, reports an excess of seven events, where 0.7 ± 0.4 are expected, with a local (global) significance of 3.6 (3.3) standard deviations. The majority of these events are reconstructed as muons candidates. However, the β values measured in the muon chambers or in the calorimeter for these seven events are compatible with 1, indicating that none of them are moving significantly slower than the speed of light.

The analysis presented here is a model-independent search for singly and doubly charged HSCPs using data collected with the CMS detector at $\sqrt{s} = 13$ TeV in 2017–2018 corresponding to an integrated luminosity of 101 fb^{-1}. In addition to an event sample significantly larger than the one in ref. [33], this search benefits from the development of a new ionization discriminator that uses the charge collected in the new Phase-1 pixel detector [35], as well as two data-driven methods to estimate the background contribution.

The paper is organized as follows. The CMS detector and event reconstruction are presented in section 2. Section 3 describes the different models considered and the associated signal samples, while section 4 introduces the ionization variables used in this search. The event selection is detailed in section 5, followed by the description of the two different background estimation methods in section 6. Section 7 presents the systematic uncertainties associated with the signals and results are shown in section 8. The paper is summarized in section 9.

Tabulated results are provided in the HEPData record for this analysis [36].

2 The CMS detector and event reconstruction

The central feature of the CMS apparatus is a superconducting solenoid of 6 m internal diameter, providing a magnetic field of 3.8 T. Within the solenoid volume are a silicon pixel and silicon strip tracker, a lead tungstate crystal electromagnetic calorimeter (ECAL), and a brass and scintillator hadron calorimeter (HCAL), each composed of a barrel and two endcap sections. Forward calorimeters extend the pseudorapidity (η) coverage provided by the barrel and endcap detectors. Muons are measured in gas-ionization detectors embedded in the steel flux-return yoke outside the solenoid. A more detailed description of the CMS detector, together with a definition of the coordinate system used and the relevant kinematic variables, can be found in ref. [37].

At the start of 2017, a new silicon pixel detector was installed [35]; the upgraded tracker measures particles up to $|\eta| < 3.0$. During the LHC running period when the data used in this paper were recorded, the silicon tracker consisted of 1856 silicon pixel and 15 148 silicon strip detector modules. In this paper, to ensure a uniform detector performance, we focus on $\mathrm{d}E/\mathrm{d}x$ measurements in the barrel part of the tracker, composed of four layers in

JHEP04(2025)109

the silicon pixel detector and 10 layers in the silicon strip detector (among which four of them are stereo, providing two separate dE/dx measurements per layer). Isolated particles of $p_T = 100\,\text{GeV}$ emitted at $|\eta| < 1.4$ have track resolutions of 2.8% in p_T and 10 (30) μm in the transverse (longitudinal) impact parameter [38]. The primary vertex is taken to be the vertex corresponding to the hardest scattering in the event, evaluated using tracking information alone, as described in section 9.4.1 of ref. [39].

Events of interest are selected using a two-tiered trigger system. The first level, composed of custom hardware processors, uses information from the calorimeters and muon detectors to select events at a rate of around 100 kHz within a fixed latency of about 4 μs [40]. The second level, known as the high-level trigger, consists of a farm of processors running a version of the full event reconstruction software optimized for fast processing, and reduces the event rate to around 1 kHz before data storage [41].

A particle flow (PF) algorithm [42] aims to reconstruct and identify each individual particle in an event, with an optimized combination of information from the various elements of the CMS detector. The energy of photons is obtained from the ECAL measurement. The energy of electrons is determined from a combination of the electron momentum at the primary interaction vertex as determined by the tracker, the energy of the corresponding ECAL cluster, and the energy sum of all bremsstrahlung photons spatially compatible with originating from the electron track. The energy of muons is obtained from the curvature of the corresponding track. The energy of charged hadrons is determined from a combination of their momentum measured in the tracker and the matching ECAL and HCAL energy deposits, corrected for the response function of the calorimeters to hadronic showers. Finally, the energy of neutral hadrons is obtained from the corresponding corrected ECAL and HCAL energies.

3 Simulated samples

This model-independent search is sensitive to a wide variety of new physics models that produce long-lived, charged particles. Several signal models are used to interpret the results. The PYTHIA generator v8.240 [43], with the tune CP5 [44] and the parton distribution function set NNPDF3.1 [45], is used to produce the Monte Carlo (MC) signal samples at $\sqrt{s} = 13\,\text{TeV}$.

The first type of signal consists of HSCPs that are charged under the strong force and live longer than typical hadronization scales. Such particles will therefore hadronize into a color-singlet hadronic state by picking up SM quarks or gluons. The pair production of long-lived gluinos ($\widetilde{g}$) is a common signature of mini-split supersymmetric (SUSY) models [46] where the decay of the $\widetilde{g}$ into a scalar squark $\widetilde{q}$, a supersymmetric partner of an SM quark, is forbidden because the $\widetilde{q}$ mass is much higher than the $\widetilde{g}$ mass. The $\widetilde{g}$ decay can then only occur via a highly virtual $\widetilde{q}$, leading to a long-lived $\widetilde{g}$ [9]. In this analysis, a quasi-stable $\widetilde{g}$ is assumed and no $\widetilde{g}$ decay is considered, corresponding to a sufficiently large scalar mass scale [47–50].

In addition, signals are available with a quasi-stable $\widetilde{t}$, the supersymmetric partner of the top quark, with masses ranging from 400 to 2600 GeV. These signals can arise, for example, in R-parity violating SUSY scenarios [51, 52]. For purposes of this study, we use long-lived $\widetilde{g}$ and $\widetilde{t}$ hadronized into R-hadrons [2, 3]. The fraction, f, of produced $\widetilde{g}$ hadronizing into a $\widetilde{g}$-gluon state (R-gluinoball) is a free parameter of the hadronization model and affects the fraction of R-hadrons that are neutral at production. The results of this search are

JHEP04(2025)109

interpreted with $f = 0.1$ to allow comparisons with previous versions of this analysis. The R-hadron's interactions with matter follow the model in refs. [53, 54].

The second type of signal consists of HSCPs that behave like leptons. Supersymmetric models featuring gauge mediated SUSY breaking (GMSB) [55] or general gauge mediation [56] commonly result in long-lived charged sleptons whose decay depends on the SUSY-breaking scale. A long-lived tau slepton ($\widetilde{\tau}$) would traverse the detector in a similar way to a slow muon. Production of $\widetilde{\tau}$ particles at the LHC can occur either directly or in the decays of heavier supersymmetric particles (mainly $\widetilde{q}$ and $\widetilde{g}$). The GMSB model is explored using the Snowmass points and slopes line 7 (SPS7) [57], which has the $\widetilde{\tau}$ as the next-to-lightest SUSY particle. The particle mass spectrum and the decay table are calculated with the program ISASUGRA [58] v7.69. The GMSB parameter Λ is the effective supersymmetry breaking scale and is varied with fixed parameters for the number of messenger particles, $N_{\text{mes}} = 3$, and their mass scale $M_{\text{mes}}/\Lambda = 2$. The ratio of the vacuum expectation values of the Higgs doublets, $\tan\beta$, is set to 10, while the sign of the higgsino mass term, μ, is assumed to be positive. We set the scale factor of the gravitino coupling, $C_{\text{grav}} = 10^4$. The large value of C_{grav} results in a long-lived $\widetilde{\tau}$, while $\Lambda = 31$–160 TeV gives a $\widetilde{\tau}$ mass of 200–1600 GeV. Two $\widetilde{\tau}$ samples are generated for each set of SUSY parameters: one with all processes (labeled "GMSB SPS7, $\widetilde{\tau}$ NLSP") and one with only direct, DY pair production (labeled "DY $\widetilde{\tau}$"). For direct pair production, different possible $\widetilde{\tau}_{\text{R}}$ and $\widetilde{\tau}_{\text{L}}$ mixing assumptions are considered.

The third type of signal is based on modified Drell-Yan (DY) production of long-lived lepton-like fermions (τ'). In this scenario, new massive spin-1/2 particles have arbitrary electric charge but are neutral under $\text{SU}(3)_C$ and $\text{SU}(2)_L$, and therefore couple only to the photon and the Z boson. Simulated samples for τ' fermions are produced with masses ranging from 200 to 2600 GeV and for electric charges $Q = 1e$ and $2e$.

The last type of signal considered originates from the proposal in ref. [59] as a possible explanation for the ATLAS excess. The proposed signature is considered using a minimal simplified model with the production of a heavy Z' boson decaying into two doubly charged τ' fermions. Limits are set on the cross section for this simplified model, and no assumption is made about the coupling structure of the Z' boson. The Z'_ψ and Z'_{SSM} production cross sections are used as benchmarks in the interpretation. The mass of the Z' boson (τ' fermion) is considered in the range 3000–7000 (200–1400) GeV.

The response of the CMS detector is simulated with the GEANT4 [60] package. The simulated events are reconstructed using the same algorithms that are used for data. In all signal samples, simulated minimum bias events are overlaid with the primary collision to produce the effect of additional interactions in the same or adjacent beam crossing (pileup) [61].

Although the background estimate performed in this search is purely data-driven, a set of MC samples for W + jets, top quark pair ($\text{t}\bar{\text{t}}$), and quantum chromodynamics (QCD) multijet production has been used to guide the selection criteria and understand qualitatively the nature of surviving background events.

4 Ionization observables

Ionization observables are based on the cluster charges deposited in the silicon pixel or strip detector [38, 62]. Dedicated corrections and filters are applied. In the strip tracker, the collected charges are corrected first by a gain calibration to stabilize the values over time by adjusting the most probable value of the charge to the energy loss by an MIP. A special correction is applied to estimate the charge deposited by the particle in case of saturation of the electronics. To reduce the rate of contamination from clusters with large energy deposition due to overlapping tracks that could occur at high pileup or in boosted hadron decay, a cleaning procedure is applied to remove clusters in the silicon strip tracker that are not consistent with the passage of a single charged particle. Strip clusters presenting a structure with multiple peaks in the distribution of the charge deposits along the strips are rejected to be consistent with the hypothesis of a single-particle deposit. Furthermore, it is required that the clusters are not located on the edge of a module in order to avoid biased measurements. These two last criteria are referred to as the "cluster cleaning". In the pixel detector, clusters are included in the ionization observable only if they are not positioned along the edges of pixel sensors, do not span two read-out chips, and do not correspond to known defective pixel channels.

A $\mathrm{d}E/\mathrm{d}x$ discriminant, $G_{\mathrm{i}}^{\mathrm{Strips}}$, is used to distinguish SM particles from HSCP candidates [30, 32, 33, 63]. Only silicon strip tracker clusters are considered in the discriminant, which is given by eq. (4.1),

$$G_{\mathrm{i}}^{\mathrm{Strips}} = \frac{3}{N}\left(\frac{1}{12N} + \sum_{j=1}^{N}\left[P_j\left(P_j - \frac{2j-1}{2N}\right)^2\right]\right), \tag{4.1}$$

where N is the number of measurements in the silicon strip detectors, P_j is the probability for an MIP with the observed path length in the detector to produce a charge smaller or equal to that of the j-th measurement in the detector, and the sum is over the track measurements ordered in terms of increasing P_j. The probabilities are determined using three-dimensional templates of path-length-normalized charge distributions per silicon strip detector module geometry and per path length, and as a function of the pileup. These templates are derived from data passing the same selection criteria as described in section 5 but within the momentum range of 20–48 GeV, for nine time periods covering the 2017–2018 data taking. The range was chosen to ensure that the tracks used to create the $G_{\mathrm{i}}^{\mathrm{Strips}}$ templates are representative of background tracks in this analysis.

A second $\mathrm{d}E/\mathrm{d}x$ discriminant, $F_{\mathrm{i}}^{\mathrm{Pixels}}$, which is introduced in this paper, relies only on the pixel detector information and is given by eq. (4.2),

$$F_{\mathrm{i}}^{\mathrm{Pixels}} = 1 - \prod_{j=1}^{n} P'_j \sum_{k=0}^{n-1} \frac{[-\ln(\prod_{j=1}^{n} P'_j)]^k}{k!}, \tag{4.2}$$

where n is the number of measurements in the silicon pixel detector, excluding the first barrel layer, which was unstable during the considered data-taking period, and P'_j is the angle dependent Vavilov probability that an MIP would produce a charge larger than the j-th measurement predicted by a detailed simulation (called PixelAV [64]), which includes effects from bias voltage changes, gain calibration changes, temperature, and irradiation dose. The use of Vavilov probabilities correctly handles distribution shape effects in long clusters. Since a parameterized function is used to calculate the probabilities, the method does not require large calibration samples in the tails of the distribution but can estimate the probabilities

Parameter	Data		Simulation	
(MeV/ cm)	2017	2018	2017	2018
K	2.54 ± 0.05	2.55 ± 0.05	2.50 ± 0.05	2.49 ± 0.05
C	3.14 ± 0.02	3.14 ± 0.02	3.18 ± 0.02	3.18 ± 0.02

Table 1. Summary of K and C values for data, and simulation.

of outlier events reliably. The PixelAV electric field maps are taken from ISE TCAD [65] simulations of a pixel cell that have been tuned to agree with in situ measurements of the Lorentz drift vs. substrate depth. The carrier trapping rates are determined from in situ charge versus depth measurements. The simulation also includes carrier diffusion and charge induction on the sensors. The electronics simulation includes noise, linearity, thresholds, and miscalibration. The Vavilov parameter templates have been produced 25 times over the 2017–2018 period, corresponding to an update about every $5\,\mathrm{fb}^{-1}$. Each set of parameters is checked against low-p_T data taken during the same calibration period.

Finally, the most probable value of $\mathrm{d}E/\mathrm{d}x$ for a track is estimated using the squared harmonic mean, as defined in eq. (4.3) [62], which suppresses the tails of the Landau distribution:

$$I_\mathrm{h} = \left(\frac{1}{N} \sum_{j=1}^{N} \left(\frac{\mathrm{d}E}{\mathrm{d}x_j} \right)^{-2} \right)^{-1/2}, \tag{4.3}$$

where $\mathrm{d}E/\mathrm{d}x_j$ is the charge per unit path length of the jth track measurement in the sensitive part of the silicon detector, in units of MeV/cm, and the summation is over the N measurements in the silicon strip detector.

The mass (m) of a candidate particle can be calculated [63] from its momentum (p) and I_h, based on a relationship approximating the Bethe-Bloch formula in the nonrelativistic regime as in eq. (4.4),

$$I_\mathrm{h} = K \frac{m^2}{p^2} + C, \tag{4.4}$$

where the empirical parameters K and C are determined using a sample of low-momentum particles composed of protons, kaons, and pions.

The values of K and C for the 2017 and 2018 data samples are listed in table 1. The uncertainties associated with the measurements take into account the variation of the data with time and small differences observed between different MC samples. By inverting eq. (4.4), the mass is estimated assuming a $Q = 1e$ particle.

5 Event selection

All events are selected online by a trigger requiring the reconstruction of a muon with transverse momentum $p_\mathrm{T} > 50\,\mathrm{GeV}$. An offline reconstructed muon passing "tight" identification criteria [66] must match the online reconstructed muon that triggered the event. The muon trigger is more efficient for lepton-like HSCPs (with the efficiency varying between 0.7 for a $\widetilde{\tau}$ mass of 1.2 TeV and 0.9 for a $\widetilde{\tau}$ mass of 300 GeV) than for R-hadron HSCPs (with

JHEP04(2025)109

efficiency varying between 0.074 for a $\widetilde{\mathrm{g}}$ mass of 2.6 TeV and 0.19 for a $\widetilde{\mathrm{g}}$ mass of 1 TeV). The mass dependence of the trigger efficiency is understood to arise from a β dependence: very slow particles ($\beta < 0.5$) reach the muon detectors later than the time window of the trigger. The reduced efficiency of the R-hadron HSCP compared to the $\widetilde{\tau}$ scenario arises because the R-hadron will sometimes, with a probability on the order of 60%, change charge when interacting with matter, leaving no signal in the muon chambers. In the case of the charge-suppressed R-hadron model (in which only the flip from charged to neutral R-hadron is allowed, not the reverse one), the efficiency is almost zero; this particular model is not considered for interpretation in this paper.

The HSCP candidates are required to be associated with a track reconstructed from hits in the silicon detectors. All events are required to have at least one HSCP candidate with $p_{\mathrm{T}} > 55\,\mathrm{GeV}$. The pseudorapidity range is restricted to $|\eta| < 1.0$ to ensure that the geometrical properties of the silicon sensor modules are uniform and to improve the signal to background ratio. To remove mismeasurements that could bias both the momentum and the ionization, a requirement on the p_{T} uncertainty divided by p_{T}^2 is applied: $\sigma_{p_{\mathrm{T}}}/p_{\mathrm{T}}^2 < 0.0008\,\mathrm{GeV}^{-1}$, which does not impact the signal efficiency for HSCP candidates at large mass. After cluster cleaning described in section 4, the candidate must have at least 10 measurements in the silicon tracker. Furthermore, to ensure good ionization measurement for the track, the HSCP candidates are required to have at least two measurements in the silicon pixel detector, a fraction of valid hits higher than 80%, pass quality (high purity) requirements, and possess a track fit value with $\chi^2/\mathrm{dof} < 5$. The details of these tracking criteria are explained in ref. [38]. Since the $F_{\mathrm{i}}^{\mathrm{Pixels}}$ variable is also sensitive to charges that are less than the expectation from an MIP, it can be used to remove truncated or broken clusters. Clusters can become truncated at module edges and dead regions of the detector. Dynamic readout inefficiencies can cause large clusters to break into smaller parts. Requiring $F_{\mathrm{i}}^{\mathrm{Pixels}}$ to be larger than 0.3 removes tracks with truncated and broken clusters. The magnitudes of the longitudinal and transverse impact parameters with respect to the primary vertex, d_{z} and d_{xy}, are required to be less than 0.1 cm and 0.02 cm, respectively, to reduce the contribution from pileup tracks and ensure that the track is originating from the hard collision.

Candidates must also pass isolation requirements. To remove the contribution to the background from events composed primarily of jets produced through the strong interaction, a relative mini-isolation variable $I_{\mathrm{PF}}^{\mathrm{rel}}$ based on PF objects is required to be less than 0.02, with $I_{\mathrm{PF}}^{\mathrm{rel}}$ defined as in eq. (5.1),

$$I_{\mathrm{PF}}^{\mathrm{rel}} = \frac{\left(\sum_{\Delta R < \Delta R_{\text{mini-iso}}} p_{\mathrm{T}}^{\mathrm{PF}}\right) - p_{\mathrm{T}}^{\mathrm{HSCP}}}{p_{\mathrm{T}}^{\mathrm{HSCP}}}, \tag{5.1}$$

where $p_{\mathrm{T}}^{\mathrm{HSCP}}$ indicates the p_{T} of the HSCP candidate. The sum runs over all PF charged and neutral hadrons, photons, electrons, and muons, and takes pileup into consideration as well, within a p_{T}-dependent cone selection [67] as specified in eq. (5.2),

$$\Delta R_{\text{mini-iso}} = \begin{cases} 0.2, & p_{\mathrm{T}}^{\mathrm{HSCP}} < 50\,\mathrm{GeV} \\ 10\,\mathrm{GeV}/p_{\mathrm{T}}^{\mathrm{HSCP}}, & 50\,\mathrm{GeV} < p_{\mathrm{T}}^{\mathrm{HSCP}} < 200\,\mathrm{GeV} \\ 0.05, & p_{\mathrm{T}}^{\mathrm{HSCP}} > 200\,\mathrm{GeV}. \end{cases} \tag{5.2}$$

JHEP04(2025)109

In particular, the inclusion of muons in the $I_{\mathrm{PF}}^{\mathrm{rel}}$ definition removes the case of two collimated muons, that could come for example from boosted resonances such as J/ψ, which could lead to a large $\mathrm{d}E/\mathrm{d}x$ deposit if the two muon tracks overlap. An absolute track-based mini-isolation requirement $I_{\mathrm{trk}} < 15\,\mathrm{GeV}$ is also applied, with I_{trk} defined as in eq. (5.3),

$$I_{\mathrm{trk}} = \left(\sum_{\Delta R < \Delta R_{\text{mini-iso}}} p_{\mathrm{T}}^{\mathrm{trk}} \right) - p_{\mathrm{T}}^{\mathrm{HSCP}}, \tag{5.3}$$

in which the sum runs over all tracks associated with the primary vertex that are within the mini-isolation cone. This absolute criterion on the I_{trk} isolation complements the relative $I_{\mathrm{PF}}^{\mathrm{rel}}$ selection by rejecting HSCP candidates with remnant activity close by. Such activity could induce a large $\mathrm{d}E/\mathrm{d}x$ value for the HSCP track if another track (from PU or other sources) crosses the module at the same place as the HSCP track. A last condition applied in the candidate selection, aimed at removing electrons, is the requirement $E/p < 0.3$, where E is the energy of the associated PF candidate measured by the calorimeters.

In the case when several HSCP candidates per event are present, the track with the highest I_{h} is used. Applying a looser ionization selection and categorizing events with exactly one or two candidates does not lead to any significant improvement.

The selection requirements are summarized in table 2 with the corresponding cumulative efficiencies for the data and two signal hypotheses. In data, the trigger efficiency represents the selection from the primary data set with muon triggers to the specific triggers used in this analysis.

6 Background prediction methods and dedicated signal and validation regions

Two different data-based estimation methods have been developed to predict the background yields, allowing cross checks to be made: the ionization method and the mass method.

6.1 The ionization method

The ionization method is based on two uncorrelated ionization variables $F_{\mathrm{i}}^{\mathrm{Pixels}}$ and $G_{\mathrm{i}}^{\mathrm{Strips}}$, which pertain to independent detectors. Figure 1 shows the $F_{\mathrm{i}}^{\mathrm{Pixels}}$ vs $G_{\mathrm{i}}^{\mathrm{Strips}}$ distribution for the SM background simulation (left) and the simulation of 1800 GeV mass $\widetilde{\mathrm{g}}$ R-hadron pair production (right) for candidates passing the event selection criteria described in section 5. The signal peaks in the high-$F_{\mathrm{i}}^{\mathrm{Pixels}}$ and high-$G_{\mathrm{i}}^{\mathrm{Strips}}$ corner, while for the background the distribution in $F_{\mathrm{i}}^{\mathrm{Pixels}}$ is flat, and $G_{\mathrm{i}}^{\mathrm{Strips}}$ follows a falling exponential-like shape.

Additional criteria on variables describing the ionization are applied to improve the discrimination of signal and background. The signal region (SR) of the ionization approach is defined by $F_{\mathrm{i}}^{\mathrm{Pixels}} > 0.9$, $G_{\mathrm{i}}^{\mathrm{Strips}} > 0.25$, and $p_{\mathrm{T}} > 200\,\mathrm{GeV}$. The cut on the transverse momentum strongly reduces the SM contribution while keeping the signal efficiency high. This p_{T} threshold is optimized with respect to the expected cross section upper limits. The optimization uses the full mass ranges of both the $\widetilde{\mathrm{g}}$ R-hadrons and $\widetilde{\tau}$ samples.

A fit is performed on the entire $G_{\mathrm{i}}^{\mathrm{Strips}}$ distribution ($0 \leq G_{\mathrm{i}}^{\mathrm{Strips}} \leq 1$) in two regions simultaneously: the FAIL region defined by $0.3 < F_{\mathrm{i}}^{\mathrm{Pixels}} < 0.9$ and the PASS region defined by $F_{\mathrm{i}}^{\mathrm{Pixels}} > 0.9$.

Selection criteria	Data	$\tilde{g}$ (1.8 TeV)	DY $\tilde{\tau}$ (557 GeV)
All events	1	1	1
Trigger	0.15	0.11	0.86
$p_T > 55$ GeV	0.11	0.11	0.86
$\lvert\eta\rvert < 1$	0.059	0.074	0.64
# of valid pixel hits in L2-L4 ≥ 2	0.056	0.071	0.62
Fraction of valid hits > 0.8	0.052	0.069	0.62
# of dE/dx measurements ≥ 10	0.052	0.069	0.62
High-purity track	0.052	0.069	0.62
Track χ^2/dof < 5	0.052	0.069	0.62
$d_z < 0.1$ cm	0.052	0.069	0.62
$d_{xy} < 0.02$ cm	0.048	0.069	0.62
$I_{PF}^{rel} < 0.02$	0.014	0.065	0.61
$I_{trk} < 15$ GeV	0.014	0.065	0.61
PF $E/p < 0.3$	0.014	0.064	0.61
$\sigma_{p_T}/p_T^2 < 0.0008$	0.014	0.064	0.61
$F_i^{Pixels} > 0.3$	0.011	0.064	0.60

Table 2. Cumulative selection efficiency for the data and for two signal hypotheses.

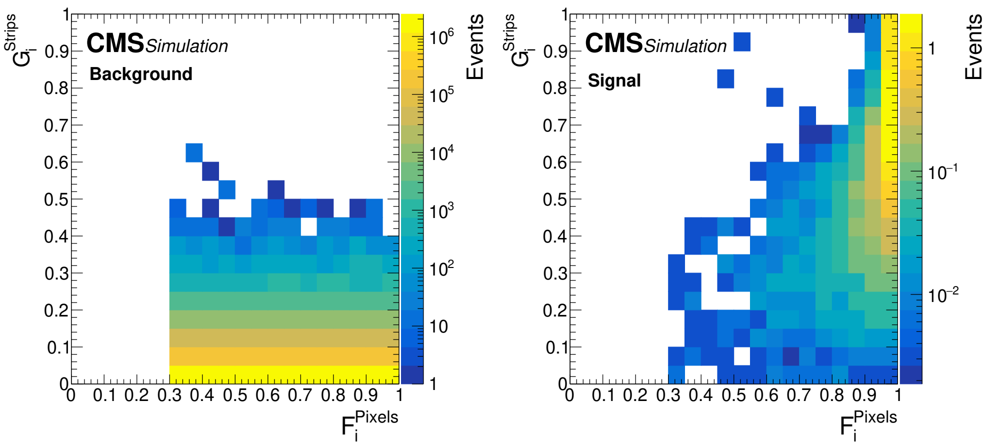

Figure 1. The simulated F_i^{Pixels} vs. G_i^{Strips} distribution for the SM background (left), and an 1800 GeV $\tilde{g}$ R-hadron (right), for events that pass the selection criteria listed in table 2.

JHEP04(2025)109

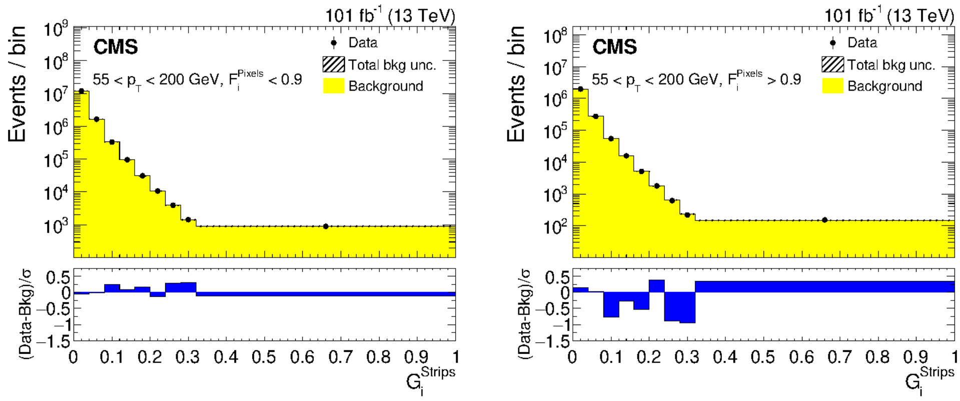

Figure 2. The $G_{\mathrm{i}}^{\mathrm{Strips}}$ distribution in the FAIL (left) and PASS (right) regions for events passing the event selection and with $55 < p_{\mathrm{T}} < 200\,\mathrm{GeV}$. The data are represented by black markers. The background predicted by the ionization method is shown in yellow, with the shaded area indicating the scarcely visible background uncertainty. The lower panel displays the pulls, defined as the difference between the data and the estimated background, divided by the associated uncertainty.

The background template used in the PASS region is estimated as the observed data distribution in the FAIL region, multiplied by a transfer function, through the relation in eq. (6.1),

$$N_{\mathrm{PASS}}^{\mathrm{bkg}}(j) = R_{\mathrm{P/F}}(j)\, N_{\mathrm{FAIL}}^{\mathrm{bkg}}(j), \tag{6.1}$$

where $N_{\mathrm{PASS}}^{\mathrm{bkg}}(j)$ is the background yield in j-th bin of the $G_{\mathrm{i}}^{\mathrm{Strips}}$ distribution in the PASS region, $N_{\mathrm{FAIL}}^{\mathrm{bkg}}(j)$ is a freely floating parameter that determines the background yield in the j-th bin, which is constrained to values close to the observed data yield during the fit, and $R_{\mathrm{P/F}}(j)$ is the value of the pass-to-fail ratio for bin j. The $R_{\mathrm{P/F}}$ ratio is modeled as a constant across the bins j, whose value is determined during the fit. Higher-order polynomials were tested using Fisher's F-test [68, 69] and provided results as good as the constant function, but not significantly better. The binning of the $G_{\mathrm{i}}^{\mathrm{Strips}}$ distribution was chosen so the last bin contains $\mathcal{O}(1)$ event in the FAIL region for the data.

The background uncertainty has two sources: the statistical uncertainty in the background yield in the FAIL region (which is dominant in the tail of the $G_{\mathrm{i}}^{\mathrm{Strips}}$ distribution) and the statistical uncertainty in $R_{\mathrm{P/F}}$.

The method is tested successfully with MC simulations and data. The validation with data is performed in two validation regions defined by lower p_{T} ranges: $50 < p_{\mathrm{T}} < 55\,\mathrm{GeV}$ and $55 < p_{\mathrm{T}} < 200\,\mathrm{GeV}$. Figure 2 shows the $G_{\mathrm{i}}^{\mathrm{Strips}}$ distribution in the FAIL and PASS regions for candidates with $55 < p_{\mathrm{T}} < 200\,\mathrm{GeV}$. The histograms associated with the 557 GeV $\widetilde{\tau}$ and 1800 GeV $\widetilde{\mathrm{g}}$ signals are not visible on these plots, their contribution being negligible in this region.

6.2 The mass method

The mass method is based on searching for a new resonance in the mass spectrum of the HSCP candidates using the ionization variable I_{h} and momentum p, calculated by inverting eq. (4.4) under the assumption $Q = 1e$ for all signals considered in this analysis. The implementation used here improves on the previously published analysis [33] in the background estimation procedure as well as in the tightened selections.

For the mass method, further requirements have been applied to the event selection in addition to those described in table 2: $I_\mathrm{h} > C$ (with C introduced in eq. (4.4)), $I_\mathrm{trk}^{\Delta R<0.3} < 15\,\mathrm{GeV}$, where the I_trk isolation variable is computed in a fixed cone of ΔR of 0.3, and $\sigma_{p_\mathrm{T}}/p_\mathrm{T} < 1$. The two last criteria reduce the background contribution in the high mass region.

The mass method relies on the lack of correlation between momentum and ionization measurements for background candidates, and divides the events into four regions:

- the control region A defined as $G_\mathrm{i}^\mathrm{Strips} < 0.018$ and $55 < p_\mathrm{T} < 70\,\mathrm{GeV}$,
- the control region B defined as $G_\mathrm{i}^\mathrm{Strips} > 0.22$ and $55 < p_\mathrm{T} < 70\,\mathrm{GeV}$,
- the control region C defined as $G_\mathrm{i}^\mathrm{Strips} < 0.018$ and $p_\mathrm{T} > 70\,\mathrm{GeV}$, and
- the signal region D is defined as $G_\mathrm{i}^\mathrm{Strips} > 0.22$ and $p_\mathrm{T} > 70\,\mathrm{GeV}$.

The fraction of events with $G_\mathrm{i}^\mathrm{Strips} > 0.22$ corresponds to approximately 0.1% of the remaining SM background, while the fraction of events with $G_\mathrm{i}^\mathrm{Strips} < 0.018$ corresponds to about 50%. The normalization of the background in signal region D ($N_{bkg}(D)$) is determined using eq. (6.2), where $N(A)$, $N(B)$, and $N(C)$ are the yields in the control regions A, B, and C, respectively.

$$N_{bkg}(D) = \frac{N(B)N(C)}{N(A)} \tag{6.2}$$

The shape of the background mass spectrum in region D comes from inverting eq. (4.4) with fitted distributions of I_h in the control region B and p in the control region C. The procedure is repeated in bins of pseudorapidity to take the correlation between p_T and p into account. In order to compute the statistical uncertainty associated to the prediction, pseudoexperiments are used in each η bin, randomizing the I_h and p templates used for the mass spectrum and the yields in the control regions for the global normalization. The average of these 200 pseudo mass-predictions is used as the central value for the mass prediction, the root mean square as the statistical uncertainty envelope.

Validation regions defined with smaller $G_\mathrm{i}^\mathrm{Strips}$ intervals (up to $G_\mathrm{i}^\mathrm{Strips} = 0.057$) are used to test the method. A trend is observed in the ratio of the observed mass spectrum to the predicted spectrum in these validation regions. The source of this effect is understood as coming from residual effects such as small nonlinear correlations between I_h and p, which are not taken into account by the method. The bias of the method is estimated by performing a fit to this ratio at low mass values $m < 300$ GeV, and used to correct the predicted mass spectrum at high mass.

Various systematic uncertainties related to the binning and the fits for the background prediction are evaluated. The largest uncertainty is associated with the bias correction, and is computed by not applying the bias correction or applying it twice.

The signal region for the mass approach is defined as $G_\mathrm{i}^\mathrm{Strips} > 0.22$, $p_\mathrm{T} > 70\,\mathrm{GeV}$, and $m > 300\,\mathrm{GeV}$. For each signal hypothesis, signal and background yields are extracted in a specific mass window defined by $[\mu - \sigma,\, \mu + 2\sigma]$ where μ is the mean of the reconstructed

JHEP04(2025)109

signal mass spectrum and σ its standard deviation. This asymmetric mass window is chosen to improve the sensitivity in the presence of a steeply falling background.

The method is extensively validated with data in validation regions at lower $G_{\mathrm{i}}^{\mathrm{Strips}}$ values, as well as with MC simulations.

6.3 Comparison of the two methods

The ionization approach selects high-ionization candidates while the mass approach selects candidates in a mass window, which allows for the acceptance of candidates with lower ionization compared to the ionization method. A study of signal MC samples shows that the overlap of the events in the SR selected by the two methods is about 60 to 80% depending on the channel. Both approaches provide similar sensitivity to the various signal processes considered here.

7 Signal systematic uncertainties

This section describes the sources of systematic uncertainty relating to the signal acceptance. The sources for the two approaches are similar.

The signal efficiencies are rescaled by the data-to-simulation correction factors for muon trigger and muon ID. The signal efficiency uncertainty is dominated by the uncertainty in the trigger efficiency for all the models. The trigger efficiency depends on the particle velocity: HSCPs that are moving too slowly could be associated with the next bunch crossing. Efficiency curves are derived as a function of the generator-level β for different bins in η, and variations on these curves have been conservatively estimated assuming a delay of 1.5 ns in the muon chambers [66]; this delay corresponds to the time resolution of the chambers. As a systematic uncertainty, β- and η-dependent trigger weights are applied to the particle that triggered the event. The impact can be as large as 30%, and is the dominant source of signal systematic uncertainty.

The stability of the $G_{\mathrm{i}}^{\mathrm{Strips}}$ variable across the data-taking period is studied. The mean of this quantity varies by about 2%. To evaluate the impact of this time variation, a smearing of the $G_{\mathrm{i}}^{\mathrm{Strips}}$ variable is applied to signal samples, and smeared samples are compared to the nominal samples without smearing. This systematic uncertainty is less than 1%.

The stability of the $F_{\mathrm{i}}^{\mathrm{Pixels}}$ variable was studied and found to be dominated by effects due to irradiation. Systematic uncertainties in the $F_{\mathrm{i}}^{\mathrm{Pixels}}$ variable are calculated using signal samples simulated with different irradiation assumptions and comparing the signal efficiency in the different cases. A change of 0.5% or less is observed when comparing the present conditions with the conditions at the beginning or at the end of the year. A conservative 0.5% systematic uncertainty is applied on the $F_{\mathrm{i}}^{\mathrm{Pixels}}$ variable, leading to a shape uncertainty.

The systematic uncertainties in the muon momentum resolution are estimated by varying the fit window and the number of bins when extracting the Z boson mass resolution, and amount to 10% of the muon momentum. Systematic uncertainties in the muon trigger efficiency, the muon identification, and the muon scale factors are also included; they lead, however, to effects less than 1%. Further details can be found in ref. [66].

The integrated luminosities for the 2017 and 2018 data taking years have 1.2–2.5% individual uncertainties [70–72], while the overall uncertainty for the 2017–2018 period is 2.0%.

JHEP04(2025)109

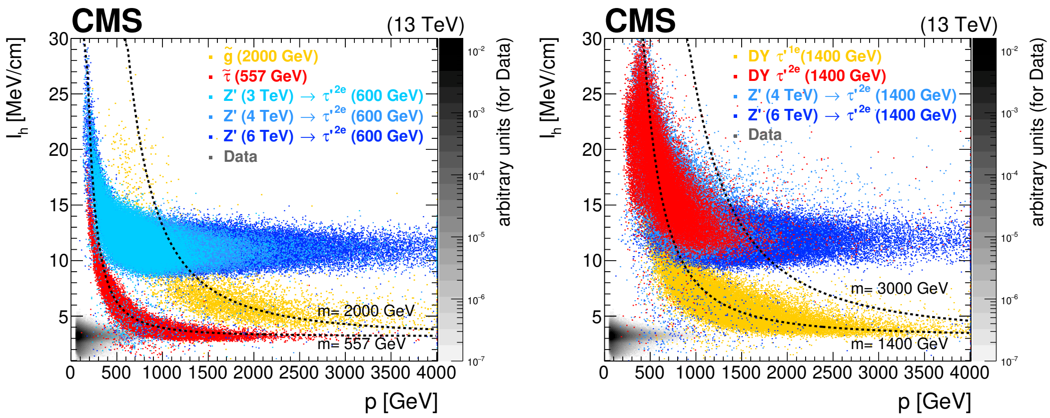

Figure 3. Distribution of I_{h} as a function of p for the HSCP candidates passing the preselection. The colored scatter plots highlight the differences between select HSCP models with various masses and charges. For illustrative purposes, observed data are displayed using the gray density distribution, normalized to unit area. The two dashed lines based on eq. (4.4) correspond to a particle mass of 557 and 2000 GeV on the left, and 1400 and 3000 GeV on the right. The momentum is measured assuming a charge $1e$.

The uncertainty in the amount of pileup is evaluated by varying the total inelastic cross section [73] used to calculate the weights by ± 1 standard deviation, then applying it to the signal events in order to reproduce the pileup distribution observed in data. The pileup uncertainty is less than 1%.

8 Results

Figure 3 shows the distribution of I_{h} as a function of p for the HSCP candidates that pass the preselection, for various signal and mass hypotheses and for data.

Figure 4 shows the $G_{\mathrm{i}}^{\mathrm{Strips}}$ distributions for the data and the predicted background with the background-only fits performed by the ionization method in the FAIL (left) and PASS (right) regions for events passing the event selection and with $p_{\mathrm{T}} > 200\,\mathrm{GeV}$. In the PASS region, one event is observed in the last bin (corresponding to $G_{\mathrm{i}}^{\mathrm{Strips}} > 0.4$) while 0.4 ± 0.2 events are expected.

Figure 5 shows the mass spectrum for the data and the predicted background for events passing the event selection, the three requirements on I_{h}, $I_{\mathrm{trk}}^{\Delta R<0.3}$, and $\sigma_{p_{\mathrm{T}}}/p_{\mathrm{T}}$ of the mass method, and the requirements on $G_{\mathrm{i}}^{\mathrm{Strips}}$ and p_{T} defining the SR: $G_{\mathrm{i}}^{\mathrm{Strips}} > 0.22$ and $p_{\mathrm{T}} > 70\,\mathrm{GeV}$. The prediction describes the data well for masses larger than 300 GeV.

The two approaches show no significant excess in the data and their results are interpreted in the context of various HSCP signal models. The limits are calculated using the CLs criterion [74, 75] with the modified profiled likelihood ratio [76] as test statistic. It uses a lognormal model for nuisance parameters affecting the yields, and shape uncertainties were parameterized as explained in ref. [77]. Given the low yields, the test statistics distributions were estimated by generating 20000 toys for the mass method and 5000 for the ionization method. The following results have been determined using the CMS statistical analysis tool Combine [77], which is based on the RooFit [78] and RooStats [79] frameworks.

JHEP04(2025)109

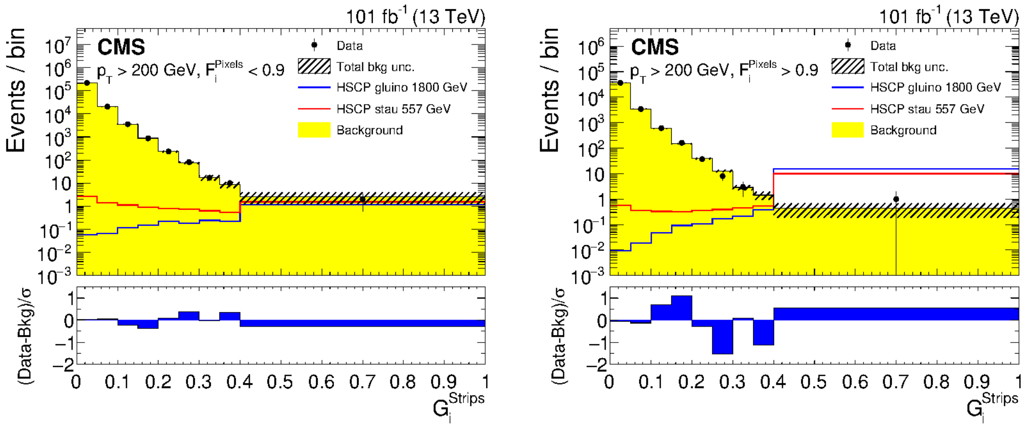

Figure 4. The $G_{\mathrm{i}}^{\mathrm{Strips}}$ distribution in the FAIL (left) and PASS (right) regions for events passing the event selection and with $p_{\mathrm{T}} > 200\,\mathrm{GeV}$. The data are represented by black dots. The background predicted by the ionization method is shown in yellow, with the hatched area indicating the background uncertainty. As examples, the blue line shows the 1800 GeV $\tilde{\mathrm{g}}$ signal distribution and the red line shows the 557 GeV $\tilde{\tau}$ signal distribution. The lower panel displays the pulls, defined as the difference between the data and the estimated background, divided by the associated uncertainty.

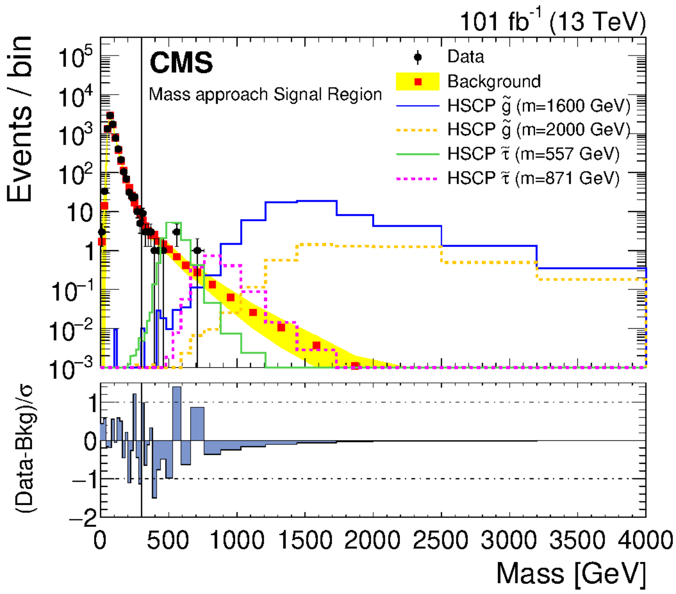

Figure 5. Mass spectrum predicted in the signal region defined by $G_{\mathrm{i}}^{\mathrm{Strips}} > 0.22$ and $p_{\mathrm{T}} > 70\,\mathrm{GeV}$. The data are represented by black dots. The data-driven background estimate is displayed as red markers with the yellow envelope representing the quadratic sum of the statistical and the systematic uncertainties. Several signal scenarios are displayed. The last bin includes the overflow. The lower panel displays the pulls, defined as the difference between the data and the estimated background, divided by the associated uncertainty.

JHEP04(2025)109

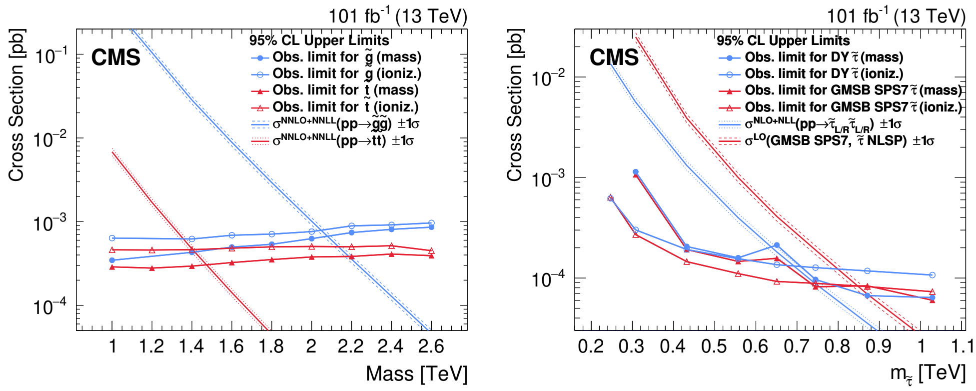

Figure 6. Cross section limits for $\tilde{g}$ (blue circles) and $\tilde{t}$ R-hadrons (red triangles) on the left and for the DY pair production of $\tilde{\tau}$ (blue circles) and within the GMSB SPS7 model (red triangles) on the right. The results obtained with the ionization method are displayed with open symbols, while the symbols for the mass method are filled. Corresponding theoretical predictions are shown using the same color code.

The mass method provides slightly stronger expected limits for signal hypotheses with a large mass because it benefits from a very low background in this regime. However, the background in the mass spectrum is not negligible below 600 GeV, degrading the limits at low masses. The ionization method, which uses the same background yield for all the signal hypothesis, performs better for low mass signals.

Figure 6 (left) shows in blue the observed upper limits on the signal production cross section for the pair production of $\tilde{g}$ R-hadrons, as a function of their mass. The cross section limits for the pair production of $\tilde{t}$ R-hadrons are displayed in red. The theoretical predictions and uncertainties for these simplified models are computed at next-to-next-to-leading order with next-to-next-to-leading logarithm resummation (NNLO+NNLL) [80–82]. At 95% CL, this search is able to exclude $\tilde{g}$ R-hadrons with a mass up to 2.06 TeV for the ionization method and up to 2.08 TeV for the mass method. The ionization (mass) method excludes $\tilde{t}$ masses below 1.40 (1.47) TeV.

This analysis is sensitive to lepton-like HSCP candidates. Limits are set on the two different $\tilde{\tau}$ production models: direct pair production of $\tilde{\tau}$ and production within the GMSB SPS7 model. The observed limits are presented in the right panel of figure 6. No mass limit can be derived below 300 GeV because of the bias correction applied in the mass method. The theoretical cross sections for direct pair production depend on the $\tilde{\tau}$ mixing parameters. However, the signal efficiency is independent of this mixing as we assume a stable $\tilde{\tau}$. Depending on the $\tilde{\tau}$ sector parameters, we are able to set three different mass limits for the ionization method (mass method): 0.52 (0.51) TeV for pair production of $\tilde{\tau}_{\mathrm{R}}$, 0.64 (0.61) TeV for pair production of $\tilde{\tau}_{\mathrm{L}}$, and 0.69 (0.64) TeV if the $\tilde{\tau}_{\mathrm{L}}$ and $\tilde{\tau}_{\mathrm{R}}$ are mass degenerate. Figure 6 (right) shows only the theoretical prediction for the last case (in blue), including both $\tilde{\tau}_{\mathrm{L}}$ and $\tilde{\tau}_{\mathrm{R}}$. In the context of the GMSB SPS7 model, $\tilde{\tau}$ masses are excluded up to 0.85 TeV for both the ionization and mass methods.

Figure 7 (left) presents the limits for the DY production of a pair of τ' leptons, assuming two different electric charge scenarios, $Q = 1e$ and $2e$, respectively. Figure 7 (right) shows

JHEP04(2025)109

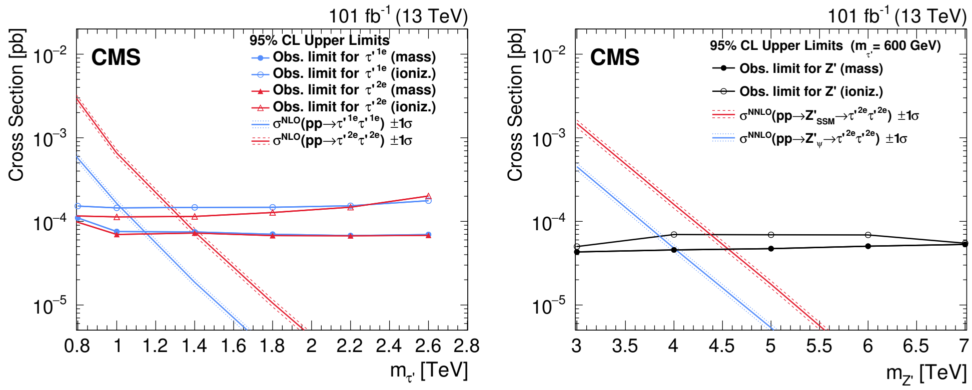

Figure 7. Cross section limits on the left for the DY-produced τ' fermions with $Q = 1e$ (blue circles) and $Q = 2e$ (red triangles), and on the right for the production of Z' boson decaying into a pair of τ' fermions of charge $2e$ (black circles). The results obtained with the ionization method are displayed with open symbols, while the symbols for the mass method are filled. The corresponding theoretical predictions for the two DY-productions are shown using the same color code as for the limits, depending on the τ' charge. For the Z' production, all the samples assume a narrow width. The branching fraction for the Z' boson decay to $\tau'\tau'$ is 1 and a fixed τ' mass of 600 GeV is used. The blue (red) curves on the right plot shows the theoretical production cross section for a Z'_ψ (Z'_{SSM}) boson [83] ([84]).

the limits for the production cross section of a Z' boson decaying into a pair of τ' fermions of charge $2e$ and a mass of 600 GeV. The theoretical cross section of production of a Z'_ψ (Z'_{SSM}) boson is taken from [83] ([84]). Drell-Yan signals with $Q = 1e$ and $2e$ are excluded below 1.02 (1.14) TeV and 1.32 (1.41) TeV for the ionization approach (for the mass method), respectively.

The mass limits obtained at $\sqrt{s} = 13$ TeV for various HSCP signal models are summarized in table 3. The observed limits on the mass are close to the expected ones. The mass method provides slightly better limits than the ionization method in the large mass regime, while the ionization method is more sensitive in the low mass regime. These results improve the exclusion mass limits compared to all previous publications.

The results for doubly charged τ' through Z' boson resonant production are shown in figure 8 as a 2D exclusion plot, taking the signal cross section for the Z' from Z'_ψ models [83, 85] and assuming a branching fraction of $Z' \to \tau'\tau'$ of 100%. This plot displays the observed cross section limit as a function of the τ' mass (on the x axis) and of the Z' boson mass (on the y axis). The empty circles correspond to the 35 simulated mass points. The cross section for the full plane is interpolated based on these 35 points. Where the Z' boson mass is 3000 GeV and each τ' has a mass of 1400 GeV, the momentum available to the τ' is very small, which makes the search less sensitive and results in higher excluded cross sections. The area above the black solid line in figure 8 corresponds to the region that is compatible with the ATLAS excess from ref. [59], while the black star corresponds to the best fit of the ATLAS excess with this model.

As the closest mass point to the star is at $m_{\tau'} = 600$ GeV, the observed exclusion limit for that particular $m_{\tau'}$ hypothesis is displayed as a function of the Z' boson mass in figure 7 (right). Limits can be set on two Z' models. The exclusion limits for the Z'_ψ model lead to an observed mass exclusion at 3.95 TeV for the ionization method and at 4.03 TeV for

Model	Ionization method		Mass method	
	Exp. (TeV)	Obs. (TeV)	Exp. (TeV)	Obs. (TeV)
$\widetilde{g}$	2.06 ± 0.06	2.06	2.08 ± 0.02	2.08
$\widetilde{t}$	1.43 ± 0.05	1.40	1.47 ± 0.02	1.47
GMSB SPS7 $\widetilde{\tau}$	0.86 ± 0.07	0.85	0.87 ± 0.05	0.85
pair-prod. $\widetilde{\tau}_R$	0.53 ± 0.03	0.52	0.50 ± 0.07	0.51
pair-prod. $\widetilde{\tau}_L$	0.66 ± 0.04	0.64	0.67 ± 0.06	0.61
pair-prod. $\widetilde{\tau}_{L/R}$	0.71 ± 0.04	0.69	0.75 ± 0.08	0.64
τ' ($Q = 1e$) from DY prod.	1.05 ± 0.05	1.02	1.14 ± 0.03	1.14
τ' ($Q = 2e$) from DY prod.	1.35 ± 0.05	1.32	1.41 ± 0.02	1.41
$Z'_\psi \to \tau'\tau'$	3.99 ± 0.21	3.95	4.03 ± 0.01	4.03
$Z'_{SSM} \to \tau'\tau'$	4.53 ± 0.23	4.38	4.56 ± 0.01	4.57

Table 3. Expected and observed mass limits obtained for various HSCP candidate models, for the two background estimate methods.

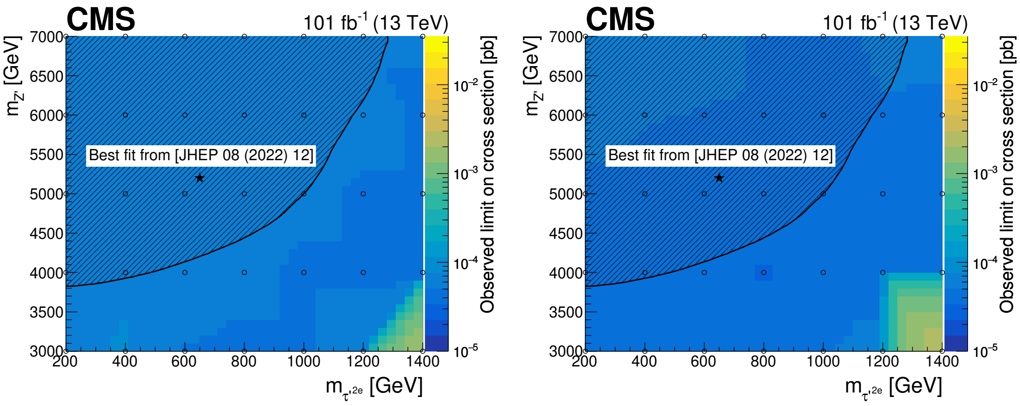

Figure 8. The two-dimensional exclusion showing the observed cross section limit as a function of the masses of the τ' (on the x axis) and of the Z' boson (on the y axis), for the ionization method on the left and for the mass method on the right. The area above the black solid line corresponds to the region that is compatible with the ATLAS excess from ref. [59] and the black star corresponds to the best fit of the ATLAS excess with this model. The empty circles correspond to the 35 simulated mass points.

the mass method. When the same signal simulation is re-interpreted for a Z' boson in the sequential SM (SSM) [84], the observed mass limit is at 4.38 TeV for the ionization method and at 4.57 TeV for the mass method. The improvement with respect to the Z'_ψ model is a consequence of the higher theoretical cross section values of the Z'_{SSM} model. The main differences between these two models are the coupling constants to the SM particles and the width of the Z' boson. The width-to-mass ratio of the Z' boson changes from 0.53% in the Z'_ψ model to 2.9% in the Z'_{SSM} model. Since these limits are set in the context of a new model, there is no direct comparison to previous results.

JHEP04(2025)109

As reported in table 5 of ref. [34], the maximum excess observed by the ATLAS Collaboration is obtained for the hypothesis of a pair production of long-lived particles with a mass of 1.4 TeV. This excess corresponds to an observed signal cross section of 0.0453 fb/($A\epsilon$). Using the acceptance (A) and efficiency (ϵ) reported in the associated HEPData record [34], this excess corresponds to an observed signal cross section of 0.59 fb under the hypothesis of a stable $\widetilde{\mathrm{g}}$. The observed excluded cross section obtained by the mass method is 0.43 fb for the same hypothesis.

In ref. [59], an interpretation for the production of a Z' boson decaying into a pair of doubly charged heavy leptons shows that masses of about 5 TeV for the Z' boson and 600 GeV for the heavy lepton could explain the ATLAS excess. For this hypothesis, the present result excludes at the 95% CL signal cross sections above 0.047 fb, and therefore does not confirm the presence of a signal excess when its corresponding ($A\epsilon$) is lower than 95%.

9 Summary

A dedicated search for heavy long-lived charged particles produced in proton-proton collisions at $\sqrt{s} = 13$ TeV using the CMS detector has been presented. Since the experimental signature is a highly ionizing isolated track of high p_{T}, the analysis is based on anomalous $\mathrm{d}E/\mathrm{d}x$ deposits in the silicon tracker. The data, corresponding to an integrated luminosity of 101 fb^{-1}, are compatible with the background predictions obtained with two different methods. The ionization method is based on the newly introduced ionization variable $F_{\mathrm{i}}^{\mathrm{Pixels}}$, which uses only pixel detector information, and the $G_{\mathrm{i}}^{\mathrm{Strips}}$ discriminant, which uses charges collected in the silicon strip detector. The mass method is based on the reconstruction of mass using the ionization variable I_{h}, providing an estimate of the most probable value of $\mathrm{d}E/\mathrm{d}x$ of the track, and the momentum of the candidate. The two methods lead to similar sensitivity. Cross section limits are set in the context of several models predicting the pair production of gluino R-hadrons, top squark R-hadrons, tau sleptons, and τ' leptons with an electric charge equal to $1e$ or $2e$. Gluino R-hadrons are excluded at the 95% CL with a mass up to 2.08 TeV, top squark R-hadrons up to 1.47 TeV, pair produced $\widetilde{\tau}_{\mathrm{L/R}}$ up to 0.69 TeV, and τ' fermions with an electric charge equal to $1e$ ($2e$) up to 1.14 (1.41) TeV. The model predicting a pair of doubly-charged τ' fermions from the Z' boson decay motivated by an excess reported by the ATLAS Collaboration [34] is directly addressed, and no significant deviation from the SM is observed. Cross section limits are extracted as a function of the Z' and τ' masses. For a τ' mass of 600 GeV, Z'_{ψ} ($\mathrm{Z}'_{\mathrm{SSM}}$) bosons are excluded at 95% CL with a mass up to 4.03 (4.57) TeV. The observed limits for stable pair produced tau sleptons, stable gluinos, and stable top squarks, as well as the Drell-Yan τ' and $\mathrm{Z}' \to \tau'\tau'$ signals are the best published to date.

Acknowledgments

We congratulate our colleagues in the CERN accelerator departments for the excellent performance of the LHC and thank the technical and administrative staffs at CERN and at other CMS institutes for their contributions to the success of the CMS effort. In addition, we gratefully acknowledge the computing centers and personnel of the Worldwide LHC Computing Grid and other centers for delivering so effectively the computing infrastructure essential to

JHEP04(2025)109

our analyses. Finally, we acknowledge the enduring support for the construction and operation of the LHC, the CMS detector, and the supporting computing infrastructure provided by the following funding agencies: SC (Armenia), BMBWF and FWF (Austria); FNRS and FWO (Belgium); CNPq, CAPES, FAPERJ, FAPERGS, and FAPESP (Brazil); MES and BNSF (Bulgaria); CERN; CAS, MoST, and NSFC (China); MINCIENCIAS (Colombia); MSES and CSF (Croatia); RIF (Cyprus); SENESCYT (Ecuador); ERC PRG, RVTT3 and MoER TK202 (Estonia); Academy of Finland, MEC, and HIP (Finland); CEA and CNRS/IN2P3 (France); SRNSF (Georgia); BMBF, DFG, and HGF (Germany); GSRI (Greece); NKFIH (Hungary); DAE and DST (India); IPM (Iran); SFI (Ireland); INFN (Italy); MSIP and NRF (Republic of Korea); MES (Latvia); LMTLT (Lithuania); MOE and UM (Malaysia); BUAP, CINVESTAV, CONACYT, LNS, SEP, and UASLP-FAI (Mexico); MOS (Montenegro); MBIE (New Zealand); PAEC (Pakistan); MES and NSC (Poland); FCT (Portugal); J MESTD (Serbia); MCIN/AEI and PCTI (Spain); MOSTR (Sri Lanka); Swiss Funding Agencies (Switzerland); MST (Taipei); MHESI and NSTDA (Thailand); TUBITAK and TENMAK (Turkey); NASU (Ukraine); STFC (United Kingdom); DOE and NSF (U.S.A.).

Individuals have received support from the Marie-Curie program and the European Research Council and Horizon 2020 Grant, contract Nos. 675440, 724704, 752730, 758316, 765710, 824093, 101115353, 101002207, and COST Action CA16108 (European Union); the Leventis Foundation; the Alfred P. Sloan Foundation; the Alexander von Humboldt Foundation; the Science Committee, project no. 22rl-037 (Armenia); the Belgian Federal Science Policy Office; the Fonds pour la Formation à la Recherche dans l'Industrie et dans l'Agriculture (FRIA-Belgium); the F.R.S.-FNRS and FWO (Belgium) under the "Excellence of Science — EOS" — be.h project n. 30820817; the Beijing Municipal Science & Technology Commission, No. Z191100007219010 and Fundamental Research Funds for the Central Universities (China); the Ministry of Education, Youth and Sports (MEYS) of the Czech Republic; the Shota Rustaveli National Science Foundation, grant FR-22-985 (Georgia); the Deutsche Forschungsgemeinschaft (DFG), among others, under Germany's Excellence Strategy — EXC 2121 "Quantum Universe" — 390833306, and under project number 400140256 — GRK2497; the Hellenic Foundation for Research and Innovation (HFRI), Project Number 2288 (Greece); the Hungarian Academy of Sciences, the New National Excellence Program — ÚNKP, the NKFIH research grants K 131991, K 133046, K 138136, K 143460, K 143477, K 146913, K 146914, K 147048, 2020-2.2.1-ED-2021-00181, and TKP2021-NKTA-64 (Hungary); the Council of Science and Industrial Research, India; ICSC — National Research Center for High Performance Computing, Big Data and Quantum Computing and FAIR — Future Artificial Intelligence Research, funded by the NextGenerationEU program (Italy); the Latvian Council of Science; the Ministry of Education and Science, project no. 2022/WK/14, and the National Science Center, contracts Opus 2021/41/B/ST2/01369 and 2021/43/B/ST2/01552 (Poland); the Fundação para a Ciência e a Tecnologia, grant CEECIND/01334/2018 (Portugal); the National Priorities Research Program by Qatar National Research Fund; MCIN/AEI/10.13039/501100011033, ERDF "a way of making Europe", and the Programa Estatal de Fomento de la Investigación Científica y Técnica de Excelencia María de Maeztu, grant MDM-2017-0765 and Programa Severo Ochoa del Principado de Asturias (Spain); the Chulalongkorn Academic into Its 2nd Century Project

JHEP04(2025)109

Advancement Project, and the National Science, Research and Innovation Fund via the Program Management Unit for Human Resources & Institutional Development, Research and Innovation, grant B39G670016 (Thailand); the Kavli Foundation; the Nvidia Corporation; the SuperMicro Corporation; the Welch Foundation, contract C-1845; and the Weston Havens Foundation (U.S.A.).

Data Availability Statement. This article has associated data in a data repository. The CMS core software is publicly available on GitHub.

Code Availability Statement. This article has associated code in a code repository. Release and preservation of data used by the CMS Collaboration as the basis for publications is guided by the CMS data preservation, re-use, and open access policy.

References

[1] M. Drees and X. Tata, *Signals for heavy exotics at hadron colliders and supercolliders*, *Phys. Lett. B* **252** (1990) 695 [INSPIRE].

[2] M. Fairbairn et al., *Stable massive particles at colliders*, *Phys. Rept.* **438** (2007) 1 [hep-ph/0611040] [INSPIRE].

[3] C.W. Bauer et al., *Supermodels for early LHC*, *Phys. Lett. B* **690** (2010) 280 [arXiv:0909.5213] [INSPIRE].

[4] A. Kusenko and M.E. Shaposhnikov, *Supersymmetric Q balls as dark matter*, *Phys. Lett. B* **418** (1998) 46 [hep-ph/9709492] [INSPIRE].

[5] B. Koch, M. Bleicher and H. Stoecker, *Black holes at LHC?*, *J. Phys. G* **34** (2007) S535 [hep-ph/0702187] [INSPIRE].

[6] J.S. Schwinger, *Magnetic charge and quantum field theory*, *Phys. Rev.* **144** (1966) 1087 [INSPIRE].

[7] D. Fargion, M. Khlopov and C.A. Stephan, *Cold dark matter by heavy double charged leptons?*, *Class. Quant. Grav.* **23** (2006) 7305 [astro-ph/0511789] [INSPIRE].

[8] J. Alimena et al., *Searching for long-lived particles beyond the Standard Model at the Large Hadron Collider*, *J. Phys. G* **47** (2020) 090501 [arXiv:1903.04497] [INSPIRE].

[9] L. Lee, C. Ohm, A. Soffer and T.-T. Yu, *Collider searches for long-lived particles beyond the Standard Model*, *Prog. Part. Nucl. Phys.* **106** (2019) 210 [*Erratum ibid.* **122** (2022) 103912] [arXiv:1810.12602] [INSPIRE].

[10] Particle Data Group collaboration, *Review of particle physics*, *Phys. Rev. D* **110** (2024) 030001 [INSPIRE].

[11] ALEPH collaboration, *Search for pair production of longlived heavy charged particles in e^+e^- annihilation*, *Phys. Lett. B* **405** (1997) 379 [hep-ex/9706013] [INSPIRE].

[12] DELPHI collaboration, *Search for heavy stable and longlived particles in e^+e^- collisions at $\sqrt{s} = 189$ GeV*, *Phys. Lett. B* **478** (2000) 65 [hep-ex/0103038] [INSPIRE].

JHEP04(2025)109

[13] L3 collaboration, *Search for heavy neutral and charged leptons in e^+e^- annihilation at LEP*, *Phys. Lett. B* **517** (2001) 75 [hep-ex/0107015] [INSPIRE].

[14] OPAL collaboration, *Search for stable and longlived massive charged particles in e^+e^- collisions at $\sqrt{s} = 130$ GeV to 209 GeV*, *Phys. Lett. B* **572** (2003) 8 [hep-ex/0305031] [INSPIRE].

[15] N. Kidonakis and R. Vogt, *Threshold corrections in bottom and charm quark hadroproduction at next-to-next-to-leading order*, *Eur. Phys. J. C* **36** (2004) 201 [hep-ph/0401056] [INSPIRE].

[16] CDF collaboration, *Search for long-lived massive charged particles in 1.96 TeV $\bar{p}p$ collisions*, *Phys. Rev. Lett.* **103** (2009) 021802 [arXiv:0902.1266] [INSPIRE].

[17] D0 collaboration, *Search for long-lived charged massive particles with the D0 detector*, *Phys. Rev. Lett.* **102** (2009) 161802 [arXiv:0809.4472] [INSPIRE].

[18] D0 collaboration, *A search for charged massive long-lived particles*, *Phys. Rev. Lett.* **108** (2012) 121802 [arXiv:1110.3302] [INSPIRE].

[19] D0 collaboration, *Search for charged massive long-lived particles at $\sqrt{s} = 1.96$ TeV*, *Phys. Rev. D* **87** (2013) 052011 [arXiv:1211.2466] [INSPIRE].

[20] ATLAS collaboration, *Search for heavy long-lived charged particles with the ATLAS detector in pp collisions at $\sqrt{s} = 7$ TeV*, *Phys. Lett. B* **703** (2011) 428 [arXiv:1106.4495] [INSPIRE].

[21] ATLAS collaboration, *Search for stable hadronising squarks and gluinos with the ATLAS experiment at the LHC*, *Phys. Lett. B* **701** (2011) 1 [arXiv:1103.1984] [INSPIRE].

[22] ATLAS collaboration, *Search for massive long-lived highly ionising particles with the ATLAS detector at the LHC*, *Phys. Lett. B* **698** (2011) 353 [arXiv:1102.0459] [INSPIRE].

[23] ATLAS collaboration, *Searches for heavy long-lived sleptons and R-hadrons with the ATLAS detector in pp collisions at $\sqrt{s} = 7$ TeV*, *Phys. Lett. B* **720** (2013) 277 [arXiv:1211.1597] [INSPIRE].

[24] ATLAS collaboration, *Search for long-lived, multi-charged particles in pp collisions at $\sqrt{s} = 7$ TeV using the ATLAS detector*, *Phys. Lett. B* **722** (2013) 305 [arXiv:1301.5272] [INSPIRE].

[25] ATLAS collaboration, *Searches for heavy long-lived charged particles with the ATLAS detector in proton-proton collisions at $\sqrt{s} = 8$ TeV*, *JHEP* **01** (2015) 068 [arXiv:1411.6795] [INSPIRE].

[26] ATLAS collaboration, *Search for heavy long-lived multi-charged particles in pp collisions at $\sqrt{s} = 8$ TeV using the ATLAS detector*, *Eur. Phys. J. C* **75** (2015) 362 [arXiv:1504.04188] [INSPIRE].

[27] ATLAS collaboration, *Search for metastable heavy charged particles with large ionisation energy loss in pp collisions at $\sqrt{s} = 8$ TeV using the ATLAS experiment*, *Eur. Phys. J. C* **75** (2015) 407 [arXiv:1506.05332] [INSPIRE].

[28] ATLAS collaboration, *Search for metastable heavy charged particles with large ionization energy loss in pp collisions at $\sqrt{s} = 13$ TeV using the ATLAS experiment*, *Phys. Rev. D* **93** (2016) 112015 [arXiv:1604.04520] [INSPIRE].

[29] ATLAS collaboration, *Search for heavy long-lived charged R-hadrons with the ATLAS detector in 3.2 fb^{-1} of proton-proton collision data at $\sqrt{s} = 13$ TeV*, *Phys. Lett. B* **760** (2016) 647 [arXiv:1606.05129] [INSPIRE].

[30] CMS collaboration, *Search for heavy stable charged particles in pp collisions at $\sqrt{s} = 7$ TeV*, *JHEP* **03** (2011) 024 [arXiv:1101.1645] [INSPIRE].

JHEP04(2025)109

- [31] CMS collaboration, *Search for fractionally charged particles in pp collisions at $\sqrt{s} = 7$ TeV*, Phys. Rev. D **87** (2013) 092008 [*Erratum ibid.* **106** (2022) 099903] [arXiv:1210.2311] [INSPIRE].
- [32] CMS collaboration, *Search for heavy long-lived charged particles in pp collisions at $\sqrt{s} = 7$ TeV*, Phys. Lett. B **713** (2012) 408 [arXiv:1205.0272] [INSPIRE].
- [33] CMS collaboration, *Search for long-lived charged particles in proton-proton collisions at $\sqrt{s} = 13$ TeV*, Phys. Rev. D **94** (2016) 112004 [arXiv:1609.08382] [INSPIRE].
- [34] ATLAS collaboration, *Search for heavy, long-lived, charged particles with large ionisation energy loss in pp collisions at $\sqrt{s} = 13$ TeV using the ATLAS experiment and the full Run 2 dataset*, JHEP **06** (2023) 158 [arXiv:2205.06013] [INSPIRE].
- [35] CMS Tracker Group collaboration, *The CMS phase-1 pixel detector upgrade*, 2021 JINST **16** P02027 [arXiv:2012.14304] [INSPIRE].
- [36] *HEPData record for this analysis*, CMS-EXO-18-002, CERN, Geneva, Switzerland (2024).
- [37] CMS collaboration, *The CMS experiment at the CERN LHC*, 2008 JINST **3** S08004 [INSPIRE].
- [38] CMS collaboration, *Description and performance of track and primary-vertex reconstruction with the CMS tracker*, 2014 JINST **9** P10009 [arXiv:1405.6569] [INSPIRE].
- [39] D. Contardo et al., *Technical proposal for the phase-II upgrade of the CMS detector*, CERN-LHCC-2015-010, CERN, Geneva, Switzerland (2015) [DOI:10.17181/CERN.VU8I.D59J].
- [40] CMS collaboration, *Performance of the CMS level-1 trigger in proton-proton collisions at $\sqrt{s} = 13$ TeV*, 2020 JINST **15** P10017 [arXiv:2006.10165] [INSPIRE].
- [41] CMS collaboration, *The CMS trigger system*, 2017 JINST **12** P01020 [arXiv:1609.02366] [INSPIRE].
- [42] CMS collaboration, *Particle-flow reconstruction and global event description with the CMS detector*, 2017 JINST **12** P10003 [arXiv:1706.04965] [INSPIRE].
- [43] T. Sjöstrand et al., *An introduction to PYTHIA 8.2*, Comput. Phys. Commun. **191** (2015) 159 [arXiv:1410.3012] [INSPIRE].
- [44] CMS collaboration, *Extraction and validation of a new set of CMS PYTHIA8 tunes from underlying-event measurements*, Eur. Phys. J. C **80** (2020) 4 [arXiv:1903.12179] [INSPIRE].
- [45] NNPDF collaboration, *Parton distributions from high-precision collider data*, Eur. Phys. J. C **77** (2017) 663 [arXiv:1706.00428] [INSPIRE].
- [46] A. Arvanitaki, N. Craig, S. Dimopoulos and G. Villadoro, *Mini-split*, JHEP **02** (2013) 126 [arXiv:1210.0555] [INSPIRE].
- [47] G.F. Giudice and A. Romanino, *Split supersymmetry*, Nucl. Phys. B **699** (2004) 65 [hep-ph/0406088] [INSPIRE].
- [48] N. Arkani-Hamed, S. Dimopoulos, G.F. Giudice and A. Romanino, *Aspects of split supersymmetry*, Nucl. Phys. B **709** (2005) 3 [hep-ph/0409232] [INSPIRE].
- [49] J.A.L. Hewett, B. Lillie, M. Masip and T.G. Rizzo, *Signatures of long-lived gluinos in split supersymmetry*, JHEP **09** (2004) 070 [hep-ph/0408248] [INSPIRE].
- [50] W. Kilian, T. Plehn, P. Richardson and E. Schmidt, *Split supersymmetry at colliders*, Eur. Phys. J. C **39** (2005) 229 [hep-ph/0408088] [INSPIRE].
- [51] C. Csáki, E. Kuflik and T. Volansky, *Dynamical R-parity violation*, Phys. Rev. Lett. **112** (2014) 131801 [arXiv:1309.5957] [INSPIRE].

JHEP04(2025)109

[52] R. Barbier et al., *R-parity violating supersymmetry*, *Phys. Rept.* **420** (2005) 1 [hep-ph/0406039] [INSPIRE].

[53] A.C. Kraan, *Interactions of heavy stable hadronizing particles*, *Eur. Phys. J. C* **37** (2004) 91 [hep-ex/0404001] [INSPIRE].

[54] R. Mackeprang and A. Rizzi, *Interactions of coloured heavy stable particles in matter*, *Eur. Phys. J. C* **50** (2007) 353 [hep-ph/0612161] [INSPIRE].

[55] G.F. Giudice and R. Rattazzi, *Theories with gauge mediated supersymmetry breaking*, *Phys. Rept.* **322** (1999) 419 [hep-ph/9801271] [INSPIRE].

[56] P. Meade, N. Seiberg and D. Shih, *General gauge mediation*, *Prog. Theor. Phys. Suppl.* **177** (2009) 143 [arXiv:0801.3278] [INSPIRE].

[57] B.C. Allanach et al., *The Snowmass points and slopes: benchmarks for SUSY searches*, *Eur. Phys. J. C* **25** (2002) 113 [hep-ph/0202233] [INSPIRE].

[58] F.E. Paige, S.D. Protopopescu, H. Baer and X. Tata, *ISAJET 7.69: a Monte Carlo event generator for pp, $\bar{p}p$, and e^+e^- reactions*, hep-ph/0312045 [INSPIRE].

[59] G.F. Giudice, M. McCullough and D. Teresi, *dE/dx from boosted long-lived particles*, *JHEP* **08** (2022) 012 [arXiv:2205.04473] [INSPIRE].

[60] GEANT4 collaboration, *GEANT4 — a simulation toolkit*, *Nucl. Instrum. Meth. A* **506** (2003) 250 [INSPIRE].

[61] CMS collaboration, *Upgrades for the CMS simulation*, *J. Phys. Conf. Ser.* **608** (2015) 012056 [INSPIRE].

[62] CMS collaboration, *CMS tracking performance results from early LHC operation*, *Eur. Phys. J. C* **70** (2010) 1165 [arXiv:1007.1988] [INSPIRE].

[63] CMS collaboration, *Searches for long-lived charged particles in pp collisions at $\sqrt{s} = 7$ and 8 TeV*, *JHEP* **07** (2013) 122 [*Erratum ibid.* **11** (2022) 149] [arXiv:1305.0491] [INSPIRE].

[64] V. Chiochia et al., *Simulation of the CMS prototype silicon pixel sensors and comparison with test beam measurements*, *IEEE Trans. Nucl. Sci.* **52** (2005) 1067 [physics/0411143] [INSPIRE].

[65] ISE Integrated Systems Engineering AG, *ISE TCAD*, release 9.0, Zürich, Switzerland (2003).

[66] CMS collaboration, *Performance of the CMS muon detector and muon reconstruction with proton-proton collisions at $\sqrt{s} = 13$ TeV*, 2018 *JINST* **13** P06015 [arXiv:1804.04528] [INSPIRE].

[67] K. Rehermann and B. Tweedie, *Efficient identification of boosted semileptonic top quarks at the LHC*, *JHEP* **03** (2011) 059 [arXiv:1007.2221] [INSPIRE].

[68] R.A. Fisher, *On the interpretation of χ^2 from contingency tables, and the calculation of p*, *J. Roy. Statist. Soc.* **85** (1922) 87.

[69] S. Baker and R.D. Cousins, *Clarification of the use of chi square and likelihood functions in fits to histograms*, *Nucl. Instrum. Meth.* **221** (1984) 437 [INSPIRE].

[70] CMS collaboration, *Precision luminosity measurement in proton-proton collisions at $\sqrt{s} = 13$ TeV in 2015 and 2016 at CMS*, *Eur. Phys. J. C* **81** (2021) 800 [arXiv:2104.01927] [INSPIRE].

[71] CMS collaboration, *CMS luminosity measurement for the 2017 data-taking period at $\sqrt{s} = 13$ TeV*, CMS-PAS-LUM-17-004, CERN, Geneva, Switzerland (2018).

[72] CMS collaboration, *CMS luminosity measurement for the 2018 data-taking period at $\sqrt{s} = 13$ TeV*, CMS-PAS-LUM-18-002, CERN, Geneva, Switzerland (2019).

JHEP04(2025)109

[73] CMS collaboration, *Measurement of the inelastic proton-proton cross section at* $\sqrt{s} = 13$ *TeV*, *JHEP* **07** (2018) 161 [arXiv:1802.02613] [INSPIRE].

[74] T. Junk, *Confidence level computation for combining searches with small statistics*, *Nucl. Instrum. Meth. A* **434** (1999) 435 [hep-ex/9902006] [INSPIRE].

[75] A.L. Read, *Presentation of search results: the* CL_s *technique*, *J. Phys. G* **28** (2002) 2693 [INSPIRE].

[76] G. Cowan, K. Cranmer, E. Gross and O. Vitells, *Asymptotic formulae for likelihood-based tests of new physics*, *Eur. Phys. J. C* **71** (2011) 1554 [*Erratum ibid.* **73** (2013) 2501] [arXiv:1007.1727] [INSPIRE].

[77] CMS collaboration, *The CMS statistical analysis and combination tool: combine*, *Comput. Softw. Big Sci.* **8** (2024) 19 [arXiv:2404.06614] [INSPIRE].

[78] W. Verkerke and D.P. Kirkby, *The RooFit toolkit for data modeling*, *eConf C* **0303241** (2003) MOLT007 [physics/0306116] [INSPIRE].

[79] L. Moneta et al., *The RooStats project*, *PoS* **ACAT2010** (2010) 057 [arXiv:1009.1003] [INSPIRE].

[80] W. Beenakker et al., *NNLL-fast: predictions for coloured supersymmetric particle production at the LHC with threshold and Coulomb resummation*, *JHEP* **12** (2016) 133 [arXiv:1607.07741] [INSPIRE].

[81] C. Borschensky et al., *Squark and gluino production cross sections in pp collisions at* $\sqrt{s} = 13, 14, 33$ *and* 100 *TeV*, *Eur. Phys. J. C* **74** (2014) 3174 [arXiv:1407.5066] [INSPIRE].

[82] J. Butterworth et al., *PDF4LHC recommendations for LHC run II*, *J. Phys. G* **43** (2016) 023001 [arXiv:1510.03865] [INSPIRE].

[83] E. Accomando et al., *Z' physics with early LHC data*, *Phys. Rev. D* **83** (2011) 075012 [arXiv:1010.6058] [INSPIRE].

[84] J.A.L. Hewett and T.G. Rizzo, *Low-energy phenomenology of superstring inspired* E_6 *models*, *Phys. Rept.* **183** (1989) 193 [INSPIRE].

[85] ATLAS collaboration, *Search for new high-mass phenomena in the dilepton final state using* $36\,fb^{-1}$ *of proton-proton collision data at* $\sqrt{s} = 13$ *TeV with the ATLAS detector*, *JHEP* **10** (2017) 182 [arXiv:1707.02424] [INSPIRE].

JHEP04(2025)109

The CMS collaboration

Yerevan Physics Institute, Yerevan, Armenia

A. Hayrapetyan, A. Tumasyan[1]

Institut für Hochenergiephysik, Vienna, Austria

W. Adam, J.W. Andrejkovic, L. Benato, T. Bergauer, S. Chatterjee, K. Damanakis, M. Dragicevic, P.S. Hussain, M. Jeitler[2], N. Krammer, A. Li, D. Liko, I. Mikulec, J. Schieck[2], R. Schöfbeck[2], D. Schwarz, M. Sonawane, W. Waltenberger, C.-E. Wulz[2]

Universiteit Antwerpen, Antwerpen, Belgium

T. Janssen, T. Van Laer, P. Van Mechelen

Vrije Universiteit Brussel, Brussel, Belgium

N. Breugelmans, J. D'Hondt, S. Dansana, A. De Moor, M. Delcourt, F. Heyen, S. Lowette, I. Makarenko, D. Müller, S. Tavernier, M. Tytgat[3], G.P. Van Onsem, S. Van Putte, D. Vannerom

Université Libre de Bruxelles, Bruxelles, Belgium

B. Bilin, B. Clerbaux, A.K. Das, I. De Bruyn, G. De Lentdecker, H. Evard, L. Favart, P. Gianneios, J. Jaramillo, A. Khalilzadeh, F.A. Khan, K. Lee, A. Malara, S. Paredes, M.A. Shahzad, L. Thomas, M. Vanden Bemden, C. Vander Velde, P. Vanlaer

Ghent University, Ghent, Belgium

M. De Coen, D. Dobur, G. Gokbulut, Y. Hong, J. Knolle, L. Lambrecht, D. Marckx, K. Mota Amarilo, K. Skovpen, N. Van Den Bossche, J. van der Linden, L. Wezenbeek

Université Catholique de Louvain, Louvain-la-Neuve, Belgium

A. Benecke, A. Bethani, G. Bruno, C. Caputo, J. De Favereau De Jeneret, C. Delaere, I.S. Donertas, A. Giammanco, A.O. Guzel, Sa. Jain, V. Lemaitre, J. Lidrych, P. Mastrapasqua, T.T. Tran

Centro Brasileiro de Pesquisas Fisicas, Rio de Janeiro, Brazil

G.A. Alves, E. Coelho, G. Correia Silva, C. Hensel, T. Menezes De Oliveira, C. Mora Herrera[4], P. Rebello Teles, M. Soeiro, A. Vilela Pereira[4]

Universidade do Estado do Rio de Janeiro, Rio de Janeiro, Brazil

W.L. Aldá Júnior, M. Barroso Ferreira Filho, H. Brandao Malbouisson, W. Carvalho, J. Chinellato[5], E.M. Da Costa, G.G. Da Silveira[6], D. De Jesus Damiao, S. Fonseca De Souza, R. Gomes De Souza, T. Laux Kuhn[6], M. Macedo, J. Martins, L. Mundim, H. Nogima, J.P. Pinheiro, A. Santoro, A. Sznajder, M. Thiel

Universidade Estadual Paulista, Universidade Federal do ABC, São Paulo, Brazil

C.A. Bernardes[6], L. Calligaris, T.R. Fernandez Perez Tomei, E.M. Gregores, I. Maietto Silverio, P.G. Mercadante, S.F. Novaes, B. Orzari, Sandra S. Padula

JHEP04(2025)109

Institute for Nuclear Research and Nuclear Energy, Bulgarian Academy of Sciences, Sofia, Bulgaria
A. Aleksandrov, G. Antchev, R. Hadjiiska, P. Iaydjiev, M. Misheva, M. Shopova, G. Sultanov

University of Sofia, Sofia, Bulgaria
A. Dimitrov, L. Litov, B. Pavlov, P. Petkov, A. Petrov, E. Shumka

Instituto De Alta Investigación, Universidad de Tarapacá, Casilla 7 D, Arica, Chile
S. Keshri, D. Laroze, S. Thakur

Beihang University, Beijing, China
T. Cheng, T. Javaid, L. Yuan

Department of Physics, Tsinghua University, Beijing, China
Z. Hu, Z. Liang, J. Liu

Institute of High Energy Physics, Beijing, China
G.M. Chen[7], H.S. Chen[7], M. Chen[7], F. Iemmi, C.H. Jiang, A. Kapoor[8], H. Liao, Z.-A. Liu[9], R. Sharma[10], J.N. Song[9], J. Tao, C. Wang[7], J. Wang, Z. Wang[7], H. Zhang, J. Zhao

State Key Laboratory of Nuclear Physics and Technology, Peking University, Beijing, China
A. Agapitos, Y. Ban, S. Deng, B. Guo, C. Jiang, A. Levin, C. Li, Q. Li, Y. Mao, S. Qian, S.J. Qian, X. Qin, X. Sun, D. Wang, H. Yang, L. Zhang, Y. Zhao, C. Zhou

Guangdong Provincial Key Laboratory of Nuclear Science and Guangdong-Hong Kong Joint Laboratory of Quantum Matter, South China Normal University, Guangzhou, China
S. Yang

Sun Yat-Sen University, Guangzhou, China
Z. You

University of Science and Technology of China, Hefei, China
K. Jaffel, N. Lu

Nanjing Normal University, Nanjing, China
G. Bauer[11], B. Li[12], K. Yi[13], J. Zhang

Institute of Modern Physics and Key Laboratory of Nuclear Physics and Ion-beam Application (MOE) — Fudan University, Shanghai, China
Y. Li

JHEP04(2025)109

Zhejiang University, Hangzhou, Zhejiang, China
Z. Lin, C. Lu, M. Xiao

Universidad de Los Andes, Bogota, Colombia
C. Avila, D.A. Barbosa Trujillo, A. Cabrera, C. Florez, J. Fraga, J.A. Reyes Vega

Universidad de Antioquia, Medellin, Colombia
F. Ramirez, C. Rendón, M. Rodriguez, A.A. Ruales Barbosa, J.D. Ruiz Alvarez

University of Split, Faculty of Electrical Engineering, Mechanical Engineering and Naval Architecture, Split, Croatia
D. Giljanovic, N. Godinovic, D. Lelas, A. Sculac

University of Split, Faculty of Science, Split, Croatia
M. Kovac, A. Petkovic, T. Sculac

Institute Rudjer Boskovic, Zagreb, Croatia
P. Bargassa, V. Brigljevic, B.K. Chitroda, D. Ferencek, K. Jakovcic, A. Starodumov[14], T. Susa

University of Cyprus, Nicosia, Cyprus
A. Attikis, K. Christoforou, A. Hadjiagapiou, C. Leonidou, J. Mousa, C. Nicolaou, L. Paizanos, F. Ptochos, P.A. Razis, H. Rykaczewski, H. Saka, A. Stepennov

Charles University, Prague, Czech Republic
M. Finger, M. Finger Jr., A. Kveton

Escuela Politecnica Nacional, Quito, Ecuador
E. Ayala

Universidad San Francisco de Quito, Quito, Ecuador
E. Carrera Jarrin

Academy of Scientific Research and Technology of the Arab Republic of Egypt, Egyptian Network of High Energy Physics, Cairo, Egypt
Y. Assran[15,16], B. El-mahdy, S. Elgammal[16]

Center for High Energy Physics (CHEP-FU), Fayoum University, El-Fayoum, Egypt
A. Lotfy, Y. Mohammed

National Institute of Chemical Physics and Biophysics, Tallinn, Estonia
K. Ehataht, M. Kadastik, T. Lange, S. Nandan, C. Nielsen, J. Pata, M. Raidal, L. Tani, C. Veelken

Department of Physics, University of Helsinki, Helsinki, Finland
H. Kirschenmann, K. Osterberg, M. Voutilainen

JHEP04(2025)109

Helsinki Institute of Physics, Helsinki, Finland
S. Bharthuar, N. Bin Norjoharuddeen, E. Brücken, F. Garcia, P. Inkaew, K.T.S. Kallonen, T. Lampén, K. Lassila-Perini, S. Lehti, T. Lindén, M. Myllymäki, M.m. Rantanen, H. Siikonen, J. Tuominiemi

Lappeenranta-Lahti University of Technology, Lappeenranta, Finland
P. Luukka, H. Petrow

IRFU, CEA, Université Paris-Saclay, Gif-sur-Yvette, France
M. Besancon, F. Couderc, M. Dejardin, D. Denegri, J.L. Faure, F. Ferri, S. Ganjour, P. Gras, G. Hamel de Monchenault, M. Kumar, V. Lohezic, J. Malcles, F. Orlandi, L. Portales, A. Rosowsky, M.Ö. Sahin, A. Savoy-Navarro[17], P. Simkina, M. Titov, M. Tornago

Laboratoire Leprince-Ringuet, CNRS/IN2P3, Ecole Polytechnique, Institut Polytechnique de Paris, Palaiseau, France
F. Beaudette, G. Boldrini, P. Busson, A. Cappati, C. Charlot, M. Chiusi, T.D. Cuisset, F. Damas, O. Davignon, A. De Wit, I.T. Ehle, B.A. Fontana Santos Alves, S. Ghosh, A. Gilbert, R. Granier de Cassagnac, A. Hakimi, B. Harikrishnan, L. Kalipoliti, G. Liu, M. Nguyen, C. Ochando, R. Salerno, J.B. Sauvan, Y. Sirois, L. Urda Gómez, E. Vernazza, A. Zabi, A. Zghiche

Université de Strasbourg, CNRS, IPHC UMR 7178, Strasbourg, France
J.-L. Agram[18], J. Andrea, D. Apparu, D. Bloch, J.-M. Brom, E.C. Chabert, C. Collard, S. Falke, U. Goerlach, R. Haeberle, A.-C. Le Bihan, M. Meena, O. Poncet, G. Saha, M.A. Sessini, P. Van Hove, P. Vaucelle

Centre de Calcul de l'Institut National de Physique Nucleaire et de Physique des Particules, CNRS/IN2P3, Villeurbanne, France
A. Di Florio

Institut de Physique des 2 Infinis de Lyon (IP2I), Villeurbanne, France
D. Amram, S. Beauceron, B. Blancon, G. Boudoul, N. Chanon, D. Contardo, P. Depasse, C. Dozen[19], H. El Mamouni, J. Fay, S. Gascon, M. Gouzevitch, C. Greenberg, G. Grenier, B. Ille, E. Jourd'huy, I.B. Laktineh, M. Lethuillier, L. Mirabito, S. Perries, A. Purohit, M. Vander Donckt, P. Verdier, J. Xiao

Georgian Technical University, Tbilisi, Georgia
D. Chokheli, I. Lomidze, Z. Tsamalaidze[14]

RWTH Aachen University, I. Physikalisches Institut, Aachen, Germany
V. Botta, S. Consuegra Rodríguez, L. Feld, K. Klein, M. Lipinski, D. Meuser, A. Pauls, D. Pérez Adán, N. Röwert, M. Teroerde

RWTH Aachen University, III. Physikalisches Institut A, Aachen, Germany
S. Diekmann, A. Dodonova, N. Eich, D. Eliseev, F. Engelke, J. Erdmann, M. Erdmann, P. Fackeldey, B. Fischer, T. Hebbeker, K. Hoepfner, F. Ivone, A. Jung,

M.y. Lee, F. Mausolf, M. Merschmeyer, A. Meyer, S. Mukherjee, D. Noll, F. Nowotny, A. Pozdnyakov, Y. Rath, W. Redjeb, F. Rehm, H. Reithler, V. Sarkisovi, A. Schmidt, C. Seth, A. Sharma, J.L. Spah, A. Stein, F. Torres Da Silva De Araujo[20], S. Wiedenbeck, S. Zaleski

RWTH Aachen University, III. Physikalisches Institut B, Aachen, Germany

C. Dziwok, G. Flügge, T. Kress, A. Nowack, O. Pooth, A. Stahl, T. Ziemons, A. Zotz

Deutsches Elektronen-Synchrotron, Hamburg, Germany

H. Aarup Petersen, M. Aldaya Martin, J. Alimena, S. Amoroso, Y. An, J. Bach, S. Baxter, M. Bayatmakou, H. Becerril Gonzalez, O. Behnke, A. Belvedere, F. Blekman[21], K. Borras[22], A. Campbell, A. Cardini, C. Cheng, F. Colombina, G. Eckerlin, D. Eckstein, L.I. Estevez Banos, E. Gallo[21], A. Geiser, V. Guglielmi, M. Guthoff, A. Hinzmann, L. Jeppe, B. Kaech, M. Kasemann, C. Kleinwort, R. Kogler, M. Komm, D. Krücker, W. Lange, D. Leyva Pernia, K. Lipka[23], W. Lohmann[24], F. Lorkowski, R. Mankel, I.-A. Melzer-Pellmann, M. Mendizabal Morentin, A.B. Meyer, G. Milella, K. Moral Figueroa, A. Mussgiller, L.P. Nair, J. Niedziela, A. Nürnberg, Y. Otarid, J. Park, E. Ranken, A. Raspereza, D. Rastorguev, J. Rübenach, L. Rygaard, A. Saggio, M. Scham[25,22], S. Schnake[22], P. Schütze, C. Schwanenberger[21], D. Selivanova, K. Sharko, M. Shchedrolosiev, D. Stafford, F. Vazzoler, A. Ventura Barroso, R. Walsh, D. Wang, Q. Wang, K. Wichmann, L. Wiens[22], C. Wissing, Y. Yang, A. Zimermmane Castro Santos

University of Hamburg, Hamburg, Germany

A. Albrecht, S. Albrecht, M. Antonello, S. Bein, S. Bollweg, M. Bonanomi, P. Connor, K. El Morabit, Y. Fischer, E. Garutti, A. Grohsjean, J. Haller, D. Hundhausen, H.R. Jabusch, G. Kasieczka, P. Keicher, R. Klanner, W. Korcari, T. Kramer, C.c. Kuo, V. Kutzner, F. Labe, J. Lange, A. Lobanov, C. Matthies, L. Moureaux, M. Mrowietz, A. Nigamova, Y. Nissan, A. Paasch, K.J. Pena Rodriguez, T. Quadfasel, B. Raciti, M. Rieger, D. Savoiu, J. Schindler, P. Schleper, M. Schröder, J. Schwandt, M. Sommerhalder, H. Stadie, G. Steinbrück, A. Tews, B. Wiederspan, M. Wolf

Karlsruher Institut fuer Technologie, Karlsruhe, Germany

S. Brommer, E. Butz, T. Chwalek, A. Dierlamm, A. Droll, U. Elicabuk, N. Faltermann, M. Giffels, A. Gottmann, F. Hartmann[26], R. Hofsaess, M. Horzela, U. Husemann, J. Kieseler, M. Klute, R. Koppenhöfer, O. Lavoryk, J.M. Lawhorn, M. Link, A. Lintuluoto, S. Maier, S. Mitra, M. Mormile, Th. Müller, M. Neukum, M. Oh, E. Pfeffer, M. Presilla, G. Quast, K. Rabbertz, B. Regnery, N. Shadskiy, I. Shvetsov, H.J. Simonis, L. Sowa, L. Stockmeier, K. Tauqeer, M. Toms, N. Trevisani, R.F. Von Cube, M. Wassmer, S. Wieland, F. Wittig, R. Wolf, X. Zuo

Institute of Nuclear and Particle Physics (INPP), NCSR Demokritos, Aghia Paraskevi, Greece

G. Anagnostou, G. Daskalakis, A. Kyriakis, A. Papadopoulos[26], A. Stakia

National and Kapodistrian University of Athens, Athens, Greece
P. Kontaxakis, G. Melachroinos, Z. Painesis, I. Papavergou, I. Paraskevas, N. Saoulidou, K. Theofilatos, E. Tziaferi, K. Vellidis, I. Zisopoulos

National Technical University of Athens, Athens, Greece
G. Bakas, T. Chatzistavrou, G. Karapostoli, K. Kousouris, I. Papakrivopoulos, E. Siamarkou, G. Tsipolitis, A. Zacharopoulou

University of Ioánnina, Ioánnina, Greece
I. Bestintzanos, I. Evangelou, C. Foudas, C. Kamtsikis, P. Katsoulis, P. Kokkas, P.G. Kosmoglou Kioseoglou, N. Manthos, I. Papadopoulos, J. Strologas

HUN-REN Wigner Research Centre for Physics, Budapest, Hungary
C. Hajdu, D. Horvath[27,28], K. Márton, A.J. Rádl[29], F. Sikler, V. Veszpremi

MTA-ELTE Lendület CMS Particle and Nuclear Physics Group, Eötvös Loránd University, Budapest, Hungary
M. Csanád, K. Farkas, A. Fehérkuti[30], M.M.A. Gadallah[31], Á. Kadlecsik, P. Major, G. Pásztor, G.I. Veres

Faculty of Informatics, University of Debrecen, Debrecen, Hungary
B. Ujvari, G. Zilizi

HUN-REN ATOMKI — Institute of Nuclear Research, Debrecen, Hungary
G. Bencze, S. Czellar, J. Molnar, Z. Szillasi

Karoly Robert Campus, MATE Institute of Technology, Gyongyos, Hungary
T. Csorgo[30], F. Nemes[30], T. Novak

Panjab University, Chandigarh, India
S. Bansal, S.B. Beri, V. Bhatnagar, G. Chaudhary, S. Chauhan, N. Dhingra[32], A. Kaur, A. Kaur, H. Kaur, M. Kaur, S. Kumar, T. Sheokand, J.B. Singh, A. Singla

University of Delhi, Delhi, India
A. Ahmed, A. Bhardwaj, A. Chhetri, B.C. Choudhary, A. Kumar, A. Kumar, M. Naimuddin, K. Ranjan, M.K. Saini, S. Saumya

Saha Institute of Nuclear Physics, HBNI, Kolkata, India
S. Baradia, S. Barman[33], S. Bhattacharya, S. Das Gupta, S. Dutta, S. Dutta, S. Sarkar

Indian Institute of Technology Madras, Madras, India
M.M. Ameen, P.K. Behera, S.C. Behera, S. Chatterjee, G. Dash, P. Jana, P. Kalbhor, S. Kamble, J.R. Komaragiri[34], D. Kumar[34], T. Mishra, B. Parida[35], P.R. Pujahari, N.R. Saha, A. Sharma, A.K. Sikdar, R.K. Singh, P. Verma, S. Verma, A. Vijay

Tata Institute of Fundamental Research-A, Mumbai, India
S. Dugad, G.B. Mohanty, M. Shelake, P. Suryadevara

JHEP04(2025)109

Tata Institute of Fundamental Research-B, Mumbai, India
A. Bala, S. Banerjee, R.M. Chatterjee, M. Guchait, Sh. Jain, A. Jaiswal, S. Kumar, G. Majumder, K. Mazumdar, S. Parolia, A. Thachayath

National Institute of Science Education and Research, An OCC of Homi Bhabha National Institute, Bhubaneswar, Odisha, India
S. Bahinipati[36], C. Kar, D. Maity[37], P. Mal, V.K. Muraleedharan Nair Bindhu[37], K. Naskar[37], A. Nayak[37], S. Nayak, K. Pal, P. Sadangi, S.K. Swain, S. Varghese[37], D. Vats[37]

Indian Institute of Science Education and Research (IISER), Pune, India
S. Acharya[38], A. Alpana, S. Dube, B. Gomber[38], P. Hazarika, B. Kansal, A. Laha, B. Sahu[38], S. Sharma, K.Y. Vaish

Isfahan University of Technology, Isfahan, Iran
H. Bakhshiansohi[39], A. Jafari[40], M. Zeinali[41]

Institute for Research in Fundamental Sciences (IPM), Tehran, Iran
S. Bashiri, S. Chenarani[42], S.M. Etesami, Y. Hosseini, M. Khakzad, E. Khazaie, M. Mohammadi Najafabadi, S. Tizchang[43]

University College Dublin, Dublin, Ireland
M. Felcini, M. Grunewald

INFN Sezione di Bari[a], Università di Bari[b], Politecnico di Bari[c], Bari, Italy
M. Abbrescia[a,b], A. Colaleo[a,b], D. Creanza[a,c], B. D'Anzi[a,b], N. De Filippis[a,c], M. De Palma[a,b], W. Elmetenawee[a,b,44], N. Ferrara[a,b], L. Fiore[a], G. Iaselli[a,c], L. Longo[a], M. Louka[a,b], G. Maggi[a,c], M. Maggi[a], I. Margjeka[a], V. Mastrapasqua[a,b], S. My[a,b], S. Nuzzo[a,b], A. Pellecchia[a,b], A. Pompili[a,b], G. Pugliese[a,c], R. Radogna[a,b], D. Ramos[a], A. Ranieri[a], L. Silvestris[a], F.M. Simone[a,c], Ü. Sözbilir[a], A. Stamerra[a,b], D. Troiano[a,b], R. Venditti[a,b], P. Verwilligen[a], A. Zaza[a,b]

INFN Sezione di Bologna[a], Università di Bologna[b], Bologna, Italy
G. Abbiendi[a], C. Battilana[a,b], D. Bonacorsi[a,b], P. Capiluppi[a,b], A. Castro[†,a,b], F.R. Cavallo[a], M. Cuffiani[a,b], G.M. Dallavalle[a], T. Diotalevi[a,b], F. Fabbri[a], A. Fanfani[a,b], D. Fasanella[a], P. Giacomelli[a], L. Giommi[a,b], C. Grandi[a], L. Guiducci[a,b], S. Lo Meo[a,45], M. Lorusso[a,b], L. Lunerti[a], S. Marcellini[a], G. Masetti[a], F.L. Navarria[a,b], G. Paggi[a,b], A. Perrotta[a], F. Primavera[a,b], A.M. Rossi[a,b], S. Rossi Tisbeni[a,b], T. Rovelli[a,b], G.P. Siroli[a,b]

INFN Sezione di Catania[a], Università di Catania[b], Catania, Italy
S. Costa[a,b,46], A. Di Mattia[a], A. Lapertosa[a], R. Potenza[a,b], A. Tricomi[a,b,46], C. Tuve[a,b]

INFN Sezione di Firenze[a], Università di Firenze[b], Firenze, Italy
P. Assiouras[a], G. Barbagli[a], G. Bardelli[a,b], B. Camaiani[a,b], A. Cassese[a], R. Ceccarelli[a], V. Ciulli[a,b], C. Civinini[a], R. D'Alessandro[a,b], E. Focardi[a,b], T. Kello[a], G. Latino[a,b],

JHEP04(2025)109

P. Lenzi[a,b], M. Lizzo[a], M. Meschini[a], S. Paoletti[a], A. Papanastassiou[a,b], G. Sguazzoni[a], L. Viliani[a]

INFN Laboratori Nazionali di Frascati, Frascati, Italy
L. Benussi, S. Bianco, S. Meola[47], D. Piccolo

INFN Sezione di Genova[a], Università di Genova[b], Genova, Italy
M. Alves Gallo Pereira[a], F. Ferro[a], E. Robutti[a], S. Tosi[a,b]

INFN Sezione di Milano-Bicocca[a], Università di Milano-Bicocca[b], Milano, Italy
A. Benaglia[a], F. Brivio[a], F. Cetorelli[a,b], F. De Guio[a,b], M.E. Dinardo[a,b], P. Dini[a], S. Gennai[a], R. Gerosa[a,b], A. Ghezzi[a,b], P. Govoni[a,b], L. Guzzi[a], M.T. Lucchini[a,b], M. Malberti[a], S. Malvezzi[a], A. Massironi[a], D. Menasce[a], L. Moroni[a], M. Paganoni[a,b], S. Palluotto[a,b], D. Pedrini[a], A. Perego[a,b], B.S. Pinolini[a], G. Pizzati[a,b], S. Ragazzi[a,b], T. Tabarelli de Fatis[a,b]

INFN Sezione di Napoli[a], Università di Napoli 'Federico II'[b], Napoli, Italy; Università della Basilicata[c], Potenza, Italy; Scuola Superiore Meridionale (SSM)[d], Napoli, Italy
S. Buontempo[a], A. Cagnotta[a,b], F. Carnevali[a,b], N. Cavallo[a,c], F. Fabozzi[a,c], A.O.M. Iorio[a,b], L. Lista[a,b,48], P. Paolucci[a,26], B. Rossi[a]

INFN Sezione di Padova[a], Università di Padova[b], Padova, Italy; Università di Trento[c], Trento, Italy
R. Ardino[a], P. Azzi[a], N. Bacchetta[a,49], D. Bisello[a,b], P. Bortignon[a], G. Bortolato[a,b], A. Bragagnolo[a,b], A.C.M. Bulla[a], R. Carlin[a,b], P. Checchia[a], T. Dorigo[a], F. Gasparini[a,b], U. Gasparini[a,b], S. Giorgetti[a], F. Gonella[a], E. Lusiani[a], M. Margoni[a,b], A.T. Meneguzzo[a,b], M. Migliorini[a,b], J. Pazzini[a,b], P. Ronchese[a,b], R. Rossin[a,b], F. Simonetto[a,b], M. Tosi[a,b], A. Triossi[a,b], S. Ventura[a], M. Zanetti[a,b], P. Zotto[a,b], A. Zucchetta[a,b]

INFN Sezione di Pavia[a], Università di Pavia[b], Pavia, Italy
A. Braghieri[a], S. Calzaferri[a], D. Fiorina[a], P. Montagna[a,b], V. Re[a], C. Riccardi[a,b], P. Salvini[a], I. Vai[a,b], P. Vitulo[a,b]

INFN Sezione di Perugia[a], Università di Perugia[b], Perugia, Italy
S. Ajmal[a,b], M.E. Ascioti[a,b], G.M. Bilei[a], C. Carrivale[a,b], D. Ciangottini[a,b], L. Fanò[a,b], M. Magherini[a,b], V. Mariani[a,b], M. Menichelli[a], F. Moscatelli[a,50], A. Rossi[a,b], A. Santocchia[a,b], D. Spiga[a], T. Tedeschi[a,b]

INFN Sezione di Pisa[a], Università di Pisa[b], Scuola Normale Superiore di Pisa[c], Pisa, Italy; Università di Siena[d], Siena, Italy
C. Aimè[a], C.A. Alexe[a,c], P. Asenov[a,b], P. Azzurri[a], G. Bagliesi[a], R. Bhattacharya[a], L. Bianchini[a,b], T. Boccali[a], E. Bossini[a], D. Bruschini[a,c], R. Castaldi[a], M.A. Ciocci[a,b], M. Cipriani[a,b], V. D'Amante[a,d], R. Dell'Orso[a], S. Donato[a], A. Giassi[a], F. Ligabue[a,c], A.C. Marini[a], D. Matos Figueiredo[a], A. Messineo[a,b], S. Mishra[a], M. Musich[a,b], F. Palla[a],

JHEP04(2025)109

A. Rizzi[a,b], G. Rolandi[a,c], S. Roy Chowdhury[a], T. Sarkar[a], A. Scribano[a], P. Spagnolo[a], R. Tenchini[a], G. Tonelli[a,b], N. Turini[a,d], F. Vaselli[a,c], A. Venturi[a], P.G. Verdini[a]

INFN Sezione di Roma[a], Sapienza Università di Roma[b], Roma, Italy

C. Baldenegro Barrera[a,b], P. Barria[a], C. Basile[a,b], F. Cavallari[a], L. Cunqueiro Mendez[a,b], D. Del Re[a,b], E. Di Marco[a,b], M. Diemoz[a], F. Errico[a,b], R. Gargiulo[a,b], E. Longo[a,b], L. Martikainen[a,b], J. Mijuskovic[a,b], G. Organtini[a,b], F. Pandolfi[a], R. Paramatti[a,b], C. Quaranta[a,b], S. Rahatlou[a,b], C. Rovelli[a], F. Santanastasio[a,b], L. Soffi[a], V. Vladimirov[a,b]

INFN Sezione di Torino[a], Università di Torino[b], Torino, Italy; Università del Piemonte Orientale[c], Novara, Italy

N. Amapane[a,b], R. Arcidiacono[a,c], S. Argiro[a,b], M. Arneodo[a,c], N. Bartosik[a], R. Bellan[a,b], A. Bellora[a,b], C. Biino[a], C. Borca[a,b], N. Cartiglia[a], M. Costa[a,b], R. Covarelli[a,b], N. Demaria[a], L. Finco[a], M. Grippo[a,b], B. Kiani[a,b], F. Legger[a], F. Luongo[a,b], C. Mariotti[a], L. Markovic[a,b], S. Maselli[a], A. Mecca[a,b], L. Menzio[a,b], P. Meridiani[a], E. Migliore[a,b], M. Monteno[a], R. Mulargia[a], M.M. Obertino[a,b], G. Ortona[a], L. Pacher[a,b], N. Pastrone[a], M. Pelliccioni[a], M. Ruspa[a,c], F. Siviero[a,b], V. Sola[a,b], A. Solano[a,b], A. Staiano[a], C. Tarricone[a,b], D. Trocino[a], G. Umoret[a,b], R. White[a,b]

INFN Sezione di Trieste[a], Università di Trieste[b], Trieste, Italy

J. Babbar[a,b], S. Belforte[a], V. Candelise[a,b], M. Casarsa[a], F. Cossutti[a], K. De Leo[a], G. Della Ricca[a,b]

Kyungpook National University, Daegu, Korea

S. Dogra, J. Hong, B. Kim, J. Kim, D. Lee, H. Lee, S.W. Lee, C.S. Moon, Y.D. Oh, M.S. Ryu, S. Sekmen, B. Tae, Y.C. Yang

Department of Mathematics and Physics — GWNU, Gangneung, Korea

M.S. Kim

Chonnam National University, Institute for Universe and Elementary Particles, Kwangju, Korea

G. Bak, P. Gwak, H. Kim, D.H. Moon

Hanyang University, Seoul, Korea

E. Asilar, J. Choi, D. Kim, T.J. Kim, J.A. Merlin, Y. Ryou

Korea University, Seoul, Korea

S. Choi, S. Han, B. Hong, K. Lee, K.S. Lee, S. Lee, J. Yoo

Kyung Hee University, Department of Physics, Seoul, Korea

J. Goh, S. Yang

Sejong University, Seoul, Korea

H. S. Kim, Y. Kim, S. Lee

JHEP04(2025)109

Seoul National University, Seoul, Korea

J. Almond, J.H. Bhyun, J. Choi, J. Choi, W. Jun, J. Kim, Y.W. Kim, S. Ko, H. Kwon, H. Lee, J. Lee, J. Lee, B.H. Oh, S.B. Oh, H. Seo, U.K. Yang, I. Yoon

University of Seoul, Seoul, Korea

W. Jang, D.Y. Kang, Y. Kang, S. Kim, B. Ko, J.S.H. Lee, Y. Lee, I.C. Park, Y. Roh, I.J. Watson

Yonsei University, Department of Physics, Seoul, Korea

S. Ha, K. Hwang, H.D. Yoo

Sungkyunkwan University, Suwon, Korea

M. Choi, M.R. Kim, H. Lee, Y. Lee, I. Yu

College of Engineering and Technology, American University of the Middle East (AUM), Dasman, Kuwait

T. Beyrouthy, Y. Gharbia

Kuwait University — College of Science — Department of Physics, Safat, Kuwait

F. Alazemi

Riga Technical University, Riga, Latvia

K. Dreimanis, A. Gaile, C. Munoz Diaz, D. Osite, G. Pikurs, A. Potrebko, M. Seidel, D. Sidiropoulos Kontos

University of Latvia (LU), Riga, Latvia

N.R. Strautnieks

Vilnius University, Vilnius, Lithuania

M. Ambrozas, A. Juodagalvis, A. Rinkevicius, G. Tamulaitis

National Centre for Particle Physics, Universiti Malaya, Kuala Lumpur, Malaysia

I. Yusuff[51], Z. Zolkapli

Universidad de Sonora (UNISON), Hermosillo, Mexico

J.F. Benitez, A. Castaneda Hernandez, H.A. Encinas Acosta, L.G. Gallegos Maríñez, M. León Coello, J.A. Murillo Quijada, A. Sehrawat, L. Valencia Palomo

Centro de Investigacion y de Estudios Avanzados del IPN, Mexico City, Mexico

G. Ayala, H. Castilla-Valdez, H. Crotte Ledesma, E. De La Cruz-Burelo, I. Heredia-De La Cruz[52], R. Lopez-Fernandez, J. Mejia Guisao, C.A. Mondragon Herrera, A. Sánchez Hernández

Universidad Iberoamericana, Mexico City, Mexico

C. Oropeza Barrera, D.L. Ramirez Guadarrama, M. Ramírez García

JHEP04(2025)109

Benemerita Universidad Autonoma de Puebla, Puebla, Mexico
I. Bautista, I. Pedraza, H.A. Salazar Ibarguen, C. Uribe Estrada

University of Montenegro, Podgorica, Montenegro
I. Bubanja, N. Raicevic

University of Canterbury, Christchurch, New Zealand
P.H. Butler

National Centre for Physics, Quaid-I-Azam University, Islamabad, Pakistan
A. Ahmad, M.I. Asghar, A. Awais, M.I.M. Awan, H.R. Hoorani, W.A. Khan

AGH University of Krakow, Krakow, Poland
V. Avati, L. Grzanka, M. Malawski

National Centre for Nuclear Research, Swierk, Poland
H. Bialkowska, M. Bluj, M. Górski, M. Kazana, M. Szleper, P. Zalewski

Institute of Experimental Physics, Faculty of Physics, University of Warsaw, Warsaw, Poland
K. Bunkowski, K. Doroba, A. Kalinowski, M. Konecki, J. Krolikowski, A. Muhammad

Warsaw University of Technology, Warsaw, Poland
P. Fokow, K. Pozniak, W. Zabolotny

Laboratório de Instrumentação e Física Experimental de Partículas, Lisboa, Portugal
M. Araujo, D. Bastos, C. Beirão Da Cruz E Silva, A. Boletti, M. Bozzo, T. Camporesi, G. Da Molin, P. Faccioli, M. Gallinaro, J. Hollar, N. Leonardo, G.B. Marozzo, A. Petrilli, M. Pisano, J. Seixas, J. Varela, J.W. Wulff

Faculty of Physics, University of Belgrade, Belgrade, Serbia
P. Adzic, P. Milenovic

VINCA Institute of Nuclear Sciences, University of Belgrade, Belgrade, Serbia
D. Devetak, M. Dordevic, J. Milosevic, L. Nadderd, V. Rekovic

Centro de Investigaciones Energéticas Medioambientales y Tecnológicas (CIEMAT), Madrid, Spain
J. Alcaraz Maestre, Cristina F. Bedoya, J.A. Brochero Cifuentes, Oliver M. Carretero, M. Cepeda, M. Cerrada, N. Colino, B. De La Cruz, A. Delgado Peris, A. Escalante Del Valle, D. Fernández Del Val, J.P. Fernández Ramos, J. Flix, M.C. Fouz, O. Gonzalez Lopez, S. Goy Lopez, J.M. Hernandez, M.I. Josa, J. Llorente Merino, C. Martin Perez, E. Martin Viscasillas, D. Moran, C. M. Morcillo Perez, Á. Navarro Tobar, C. Perez Dengra, A. Pérez-Calero Yzquierdo, J. Puerta Pelayo, I. Redondo, S. Sánchez Navas, J. Sastre, J. Vazquez Escobar

JHEP04(2025)109

Universidad Autónoma de Madrid, Madrid, Spain
J.F. de Trocóniz

Universidad de Oviedo, Instituto Universitario de Ciencias y Tecnologías Espaciales de Asturias (ICTEA), Oviedo, Spain
B. Alvarez Gonzalez, J. Cuevas, J. Fernandez Menendez, S. Folgueras, I. Gonzalez Caballero, P. Leguina, E. Palencia Cortezon, J. Prado Pico, C. Ramón Álvarez, V. Rodríguez Bouza, A. Soto Rodríguez, A. Trapote, C. Vico Villalba, P. Vischia

Instituto de Física de Cantabria (IFCA), CSIC-Universidad de Cantabria, Santander, Spain
S. Bhowmik, S. Blanco Fernández, I.J. Cabrillo, A. Calderon, J. Duarte Campderros, M. Fernandez, G. Gomez, C. Lasaosa García, R. Lopez Ruiz, C. Martinez Rivero, P. Martinez Ruiz del Arbol, F. Matorras, P. Matorras Cuevas, E. Navarrete Ramos, J. Piedra Gomez, L. Scodellaro, I. Vila, J.M. Vizan Garcia

University of Colombo, Colombo, Sri Lanka
B. Kailasapathy[53], D.D.C. Wickramarathna

University of Ruhuna, Department of Physics, Matara, Sri Lanka
W.G.D. Dharmaratna[54], K. Liyanage, N. Perera

CERN, European Organization for Nuclear Research, Geneva, Switzerland
D. Abbaneo, C. Amendola, E. Auffray, G. Auzinger, J. Baechler, D. Barney, A. Bermúdez Martínez, M. Bianco, A.A. Bin Anuar, A. Bocci, L. Borgonovi, C. Botta, E. Brondolin, C. Caillol, G. Cerminara, N. Chernyavskaya, D. d'Enterria, A. Dabrowski, A. David, A. De Roeck, M.M. Defranchis, M. Deile, M. Dobson, G. Franzoni, W. Funk, S. Giani, D. Gigi, K. Gill, F. Glege, J. Hegeman, J.K. Heikkilä, B. Huber, V. Innocente, T. James, P. Janot, O. Kaluzinska, O. Karacheban[24], S. Laurila, P. Lecoq, E. Leutgeb, C. Lourenço, L. Malgeri, M. Mannelli, M. Matthewman, A. Mehta, F. Meijers, S. Mersi, E. Meschi, V. Milosevic, F. Monti, F. Moortgat, M. Mulders, I. Neutelings, S. Orfanelli, F. Pantaleo, G. Petrucciani, A. Pfeiffer, M. Pierini, H. Qu, D. Rabady, B. Ribeiro Lopes, F. Riti, M. Rovere, H. Sakulin, R. Salvatico, S. Sanchez Cruz, S. Scarfi, C. Schwick, M. Selvaggi, A. Sharma, K. Shchelina, P. Silva, P. Sphicas[55], A.G. Stahl Leiton, A. Steen, S. Summers, D. Treille, P. Tropea, D. Walter, J. Wanczyk[56], J. Wang, K.A. Wozniak[57], S. Wuchterl, P. Zehetner, P. Zejdl, W.D. Zeuner

Paul Scherrer Institut, Villigen, Switzerland
T. Bevilacqua[58], L. Caminada[58], A. Ebrahimi, W. Erdmann, R. Horisberger, Q. Ingram, H.C. Kaestli, D. Kotlinski, C. Lange, M. Missiroli[58], L. Noehte[58], T. Rohe, A. Samalan

ETH Zurich — Institute for Particle Physics and Astrophysics (IPA), Zurich, Switzerland
T.K. Aarrestad, M. Backhaus, G. Bonomelli, A. Calandri, C. Cazzaniga, K. Datta, P. De Bryas Dexmiers D'archiac[56], A. De Cosa, G. Dissertori, M. Dittmar, M. Donegà,

JHEP04(2025)109

F. Eble, M. Galli, K. Gedia, F. Glessgen, C. Grab, N. Härringer, T.G. Harte, D. Hits, W. Lustermann, A.-M. Lyon, R.A. Manzoni, M. Marchegiani, L. Marchese, A. Mascellani[56], F. Nessi-Tedaldi, F. Pauss, V. Perovic, S. Pigazzini, B. Ristic, R. Seidita, J. Steggemann[56], A. Tarabini, D. Valsecchi, R. Wallny

Universität Zürich, Zurich, Switzerland
C. Amsler[59], P. Bärtschi, M.F. Canelli, K. Cormier, M. Huwiler, W. Jin, A. Jofrehei, B. Kilminster, S. Leontsinis, S.P. Liechti, A. Macchiolo, P. Meiring, F. Meng, J. Motta, A. Reimers, P. Robmann, M. Senger, E. Shokr, F. Stäger, R. Tramontano

National Central University, Chung-Li, Taiwan
C. Adloff[60], D. Bhowmik, C.M. Kuo, W. Lin, P.K. Rout, P.C. Tiwari[34]

National Taiwan University (NTU), Taipei, Taiwan
L. Ceard, K.F. Chen, Z.g. Chen, A. De Iorio, W.-S. Hou, T.h. Hsu, Y.w. Kao, S. Karmakar, G. Kole, Y.y. Li, R.-S. Lu, E. Paganis, X.f. Su, J. Thomas-Wilsker, L.s. Tsai, D. Tsionou, H.y. Wu, E. Yazgan

High Energy Physics Research Unit, Department of Physics, Faculty of Science, Chulalongkorn University, Bangkok, Thailand
C. Asawatangtrakuldee, N. Srimanobhas, V. Wachirapusitanand

Çukurova University, Physics Department, Science and Art Faculty, Adana, Turkey
D. Agyel, F. Boran, F. Dolek, I. Dumanoglu[61], E. Eskut, Y. Guler[62], E. Gurpinar Guler[62], C. Isik, O. Kara, A. Kayis Topaksu, U. Kiminsu, Y. Komurcu, G. Onengut, K. Ozdemir[63], A. Polatoz, B. Tali[64], U.G. Tok, S. Turkcapar, E. Uslan, I.S. Zorbakir

Middle East Technical University, Physics Department, Ankara, Turkey
G. Sokmen, M. Yalvac[65]

Bogazici University, Istanbul, Turkey
B. Akgun, I.O. Atakisi, E. Gülmez, M. Kaya[66], O. Kaya[67], S. Tekten[68]

Istanbul Technical University, Istanbul, Turkey
A. Cakir, K. Cankocak[61,69], G.G. Dincer[61], S. Sen[70]

Istanbul University, Istanbul, Turkey
O. Aydilek[71], B. Hacisahinoglu, I. Hos[72], B. Kaynak, S. Ozkorucuklu, O. Potok, H. Sert, C. Simsek, C. Zorbilmez

Yildiz Technical University, Istanbul, Turkey
S. Cerci, B. Isildak[73], D. Sunar Cerci, T. Yetkin

Institute for Scintillation Materials of National Academy of Science of Ukraine, Kharkiv, Ukraine
A. Boyaryntsev, B. Grynyov

National Science Centre, Kharkiv Institute of Physics and Technology, Kharkiv, Ukraine
L. Levchuk

University of Bristol, Bristol, United Kingdom
D. Anthony, J.J. Brooke, A. Bundock, F. Bury, E. Clement, D. Cussans, H. Flacher, M. Glowacki, J. Goldstein, H.F. Heath, M.-L. Holmberg, L. Kreczko, S. Paramesvaran, L. Robertshaw, V.J. Smith, K. Walkingshaw Pass

Rutherford Appleton Laboratory, Didcot, United Kingdom
A.H. Ball, K.W. Bell, A. Belyaev[74], C. Brew, R.M. Brown, D.J.A. Cockerill, C. Cooke, A. Elliot, K.V. Ellis, K. Harder, S. Harper, J. Linacre, K. Manolopoulos, D.M. Newbold, E. Olaiya, D. Petyt, T. Reis, A.R. Sahasransu, G. Salvi, T. Schuh, C.H. Shepherd-Themistocleous, I.R. Tomalin, K.C. Whalen, T. Williams

Imperial College, London, United Kingdom
I. Andreou, R. Bainbridge, P. Bloch, C.E. Brown, O. Buchmuller, C.A. Carrillo Montoya, G.S. Chahal[75], D. Colling, J.S. Dancu, I. Das, P. Dauncey, G. Davies, M. Della Negra, S. Fayer, G. Fedi, G. Hall, A. Howard, G. Iles, C.R. Knight, P. Krueper, J. Langford, K.H. Law, J. León Holgado, L. Lyons, A.-M. Magnan, B. Maier, S. Mallios, M. Mieskolainen, J. Nash[76], M. Pesaresi, P.B. Pradeep, B.C. Radburn-Smith, A. Richards, A. Rose, K. Savva, C. Seez, R. Shukla, A. Tapper, K. Uchida, G.P. Uttley, T. Virdee[26], M. Vojinovic, N. Wardle, D. Winterbottom

Brunel University, Uxbridge, United Kingdom
J.E. Cole, A. Khan, P. Kyberd, I.D. Reid

Baylor University, Waco, Texas, U.S.A.
S. Abdullin, A. Brinkerhoff, E. Collins, M.R. Darwish, J. Dittmann, K. Hatakeyama, J. Hiltbrand, B. McMaster, J. Samudio, S. Sawant, C. Sutantawibul, J. Wilson

Catholic University of America, Washington, DC, U.S.A.
R. Bartek, A. Dominguez, A.E. Simsek, S.S. Yu

The University of Alabama, Tuscaloosa, Alabama, U.S.A.
B. Bam, A. Buchot Perraguin, R. Chudasama, S.I. Cooper, C. Crovella, S.V. Gleyzer, E. Pearson, C.U. Perez, P. Rumerio[77], E. Usai, R. Yi

Boston University, Boston, Massachusetts, U.S.A.
A. Akpinar, C. Cosby, G. De Castro, Z. Demiragli, C. Erice, C. Fangmeier, C. Fernandez Madrazo, E. Fontanesi, D. Gastler, F. Golf, S. Jeon, J. O‘cain, I. Reed, J. Rohlf, K. Salyer, D. Sperka, D. Spitzbart, I. Suarez, A. Tsatsos, A.G. Zecchinelli

JHEP04(2025)109

Brown University, Providence, Rhode Island, U.S.A.
G. Barone, G. Benelli, D. Cutts, L. Gouskos, M. Hadley, U. Heintz, J.M. Hogan[78], T. Kwon, G. Landsberg, K.T. Lau, D. Li, J. Luo, S. Mondal, T. Russell, S. Sagir[79], X. Shen, F. Simpson, M. Stamenkovic, N. Venkatasubramanian, X. Yan

University of California, Davis, Davis, California, U.S.A.
S. Abbott, B. Barton, C. Brainerd, R. Breedon, H. Cai, M. Calderon De La Barca Sanchez, M. Chertok, M. Citron, J. Conway, P.T. Cox, R. Erbacher, F. Jensen, O. Kukral, G. Mocellin, M. Mulhearn, S. Ostrom, W. Wei, S. Yoo, F. Zhang

University of California, Los Angeles, California, U.S.A.
K. Adamidis, M. Bachtis, D. Campos, R. Cousins, A. Datta, G. Flores Avila, J. Hauser, M. Ignatenko, M.A. Iqbal, T. Lam, Y.f. Lo, E. Manca, A. Nunez Del Prado, D. Saltzberg, V. Valuev

University of California, Riverside, Riverside, California, U.S.A.
R. Clare, J.W. Gary, G. Hanson

University of California, San Diego, La Jolla, California, U.S.A.
A. Aportela, A. Arora, J.G. Branson, S. Cittolin, S. Cooperstein, D. Diaz, J. Duarte, L. Giannini, Y. Gu, J. Guiang, R. Kansal, V. Krutelyov, R. Lee, J. Letts, M. Masciovecchio, F. Mokhtar, S. Mukherjee, M. Pieri, M. Quinnan, B.V. Sathia Narayanan, V. Sharma, M. Tadel, E. Vourliotis, F. Würthwein, Y. Xiang, A. Yagil

University of California, Santa Barbara — Department of Physics, Santa Barbara, California, U.S.A.
A. Barzdukas, L. Brennan, C. Campagnari, K. Downham, C. Grieco, J. Incandela, J. Kim, A.J. Li, P. Masterson, H. Mei, J. Richman, S.N. Santpur, U. Sarica, R. Schmitz, F. Setti, J. Sheplock, D. Stuart, T.Á. Vámi, S. Wang, D. Zhang

California Institute of Technology, Pasadena, California, U.S.A.
S. Bhattacharya, A. Bornheim, O. Cerri, A. Latorre, J. Mao, H.B. Newman, G. Reales Gutiérrez, M. Spiropulu, J.R. Vlimant, C. Wang, S. Xie, R.Y. Zhu

Carnegie Mellon University, Pittsburgh, Pennsylvania, U.S.A.
J. Alison, S. An, P. Bryant, M. Cremonesi, V. Dutta, T. Ferguson, T.A. Gómez Espinosa, A. Harilal, A. Kallil Tharayil, C. Liu, T. Mudholkar, S. Murthy, P. Palit, K. Park, M. Paulini, A. Roberts, A. Sanchez, W. Terrill

University of Colorado Boulder, Boulder, Colorado, U.S.A.
J.P. Cumalat, W.T. Ford, A. Hart, A. Hassani, G. Karathanasis, N. Manganelli, J. Pearkes, C. Savard, N. Schonbeck, K. Stenson, K.A. Ulmer, S.R. Wagner, N. Zipper, D. Zuolo

JHEP04(2025)109

Cornell University, Ithaca, New York, U.S.A.
J. Alexander, S. Bright-Thonney, X. Chen, D.J. Cranshaw, J. Fan, X. Fan, S. Hogan, P. Kotamnives, J. Monroy, M. Oshiro, J.R. Patterson, M. Reid, A. Ryd, J. Thom, P. Wittich, R. Zou

Fermi National Accelerator Laboratory, Batavia, Illinois, U.S.A.
M. Albrow, M. Alyari, O. Amram, G. Apollinari, A. Apresyan, L.A.T. Bauerdick, D. Berry, J. Berryhill, P.C. Bhat, K. Burkett, J.N. Butler, A. Canepa, G.B. Cerati, H.W.K. Cheung, F. Chlebana, G. Cummings, J. Dickinson, I. Dutta, V.D. Elvira, Y. Feng, J. Freeman, A. Gandrakota, Z. Gecse, L. Gray, D. Green, A. Grummer, S. Grünendahl, D. Guerrero, O. Gutsche, R.M. Harris, R. Heller, T.C. Herwig, J. Hirschauer, B. Jayatilaka, S. Jindariani, M. Johnson, U. Joshi, T. Klijnsma, B. Klima, K.H.M. Kwok, S. Lammel, C. Lee, D. Lincoln, R. Lipton, T. Liu, C. Madrid, K. Maeshima, C. Mantilla, D. Mason, P. McBride, P. Merkel, S. Mrenna, S. Nahn, J. Ngadiuba, D. Noonan, S. Norberg, V. Papadimitriou, N. Pastika, K. Pedro, C. Pena[80], F. Ravera, A. Reinsvold Hall[81], L. Ristori, M. Safdari, E. Sexton-Kennedy, N. Smith, A. Soha, L. Spiegel, S. Stoynev, J. Strait, L. Taylor, S. Tkaczyk, N.V. Tran, L. Uplegger, E.W. Vaandering, I. Zoi

University of Florida, Gainesville, Florida, U.S.A.
C. Aruta, P. Avery, D. Bourilkov, P. Chang, V. Cherepanov, R.D. Field, C. Huh, E. Koenig, M. Kolosova, J. Konigsberg, A. Korytov, K. Matchev, N. Menendez, G. Mitselmakher, K. Mohrman, A. Muthirakalayil Madhu, N. Rawal, S. Rosenzweig, Y. Takahashi, J. Wang

Florida State University, Tallahassee, Florida, U.S.A.
T. Adams, A. Al Kadhim, A. Askew, S. Bower, R. Hashmi, R.S. Kim, S. Kim, T. Kolberg, G. Martinez, H. Prosper, P.R. Prova, M. Wulansatiti, R. Yohay, J. Zhang

Florida Institute of Technology, Melbourne, Florida, U.S.A.
B. Alsufyani, M.M. Baarmand, S. Butalla, S. Das, T. Elkafrawy[82], M. Hohlmann, E. Yanes

University of Illinois Chicago, Chicago, Illinois, U.S.A.
M.R. Adams, A. Baty, C. Bennett, R. Cavanaugh, R. Escobar Franco, O. Evdokimov, C.E. Gerber, M. Hawksworth, A. Hingrajiya, D.J. Hofman, J.h. Lee, D. S. Lemos, A.H. Merrit, C. Mills, S. Nanda, G. Oh, B. Ozek, D. Pilipovic, R. Pradhan, E. Prifti, T. Roy, S. Rudrabhatla, N. Singh, M.B. Tonjes, N. Varelas, M.A. Wadud, Z. Ye, J. Yoo

The University of Iowa, Iowa City, Iowa, U.S.A.
M. Alhusseini, D. Blend, K. Dilsiz[83], L. Emediato, G. Karaman, O.K. Köseyan, J.-P. Merlo, A. Mestvirishvili[84], O. Neogi, H. Ogul[85], Y. Onel, A. Penzo, C. Snyder, E. Tiras[86]

JHEP04(2025)109

Johns Hopkins University, Baltimore, Maryland, U.S.A.
B. Blumenfeld, L. Corcodilos, J. Davis, A.V. Gritsan, L. Kang, S. Kyriacou, P. Maksimovic, M. Roguljic, J. Roskes, S. Sekhar, M. Swartz

The University of Kansas, Lawrence, Kansas, U.S.A.
A. Abreu, L.F. Alcerro Alcerro, J. Anguiano, S. Arteaga Escatel, P. Baringer, A. Bean, Z. Flowers, D. Grove, J. King, G. Krintiras, M. Lazarovits, C. Le Mahieu, J. Marquez, M. Murray, M. Nickel, M. Pitt, S. Popescu[87], C. Rogan, C. Royon, S. Sanders, C. Smith, G. Wilson

Kansas State University, Manhattan, Kansas, U.S.A.
B. Allmond, R. Gujju Gurunadha, A. Ivanov, K. Kaadze, Y. Maravin, J. Natoli, D. Roy, G. Sorrentino

University of Maryland, College Park, Maryland, U.S.A.
A. Baden, A. Belloni, J. Bistany-riebman, Y.M. Chen, S.C. Eno, N.J. Hadley, S. Jabeen, R.G. Kellogg, T. Koeth, B. Kronheim, Y. Lai, S. Lascio, A.C. Mignerey, S. Nabili, C. Palmer, C. Papageorgakis, M.M. Paranjpe, E. Popova[88], A. Shevelev, L. Wang

Massachusetts Institute of Technology, Cambridge, Massachusetts, U.S.A.
J. Bendavid, I.A. Cali, P.c. Chou, M. D'Alfonso, J. Eysermans, C. Freer, G. Gomez-Ceballos, M. Goncharov, G. Grosso, P. Harris, D. Hoang, D. Kovalskyi, J. Krupa, L. Lavezzo, Y.-J. Lee, K. Long, C. Mcginn, A. Novak, M.I. Park, C. Paus, C. Reissel, C. Roland, G. Roland, S. Rothman, G.S.F. Stephans, Z. Wang, B. Wyslouch, T. J. Yang

University of Minnesota, Minneapolis, Minnesota, U.S.A.
B. Crossman, B.M. Joshi, C. Kapsiak, M. Krohn, D. Mahon, J. Mans, B. Marzocchi, M. Revering, R. Rusack, R. Saradhy, N. Strobbe

University of Nebraska-Lincoln, Lincoln, Nebraska, U.S.A.
K. Bloom, D.R. Claes, G. Haza, J. Hossain, C. Joo, I. Kravchenko, J.E. Siado, W. Tabb, A. Vagnerini, A. Wightman, F. Yan, D. Yu

State University of New York at Buffalo, Buffalo, New York, U.S.A.
H. Bandyopadhyay, L. Hay, H.w. Hsia, I. Iashvili, A. Kalogeropoulos, A. Kharchilava, M. Morris, D. Nguyen, S. Rappoccio, H. Rejeb Sfar, A. Williams, P. Young

Northeastern University, Boston, Massachusetts, U.S.A.
G. Alverson, E. Barberis, J. Bonilla, B. Bylsma, M. Campana, J. Dervan, Y. Haddad, Y. Han, I. Israr, A. Krishna, J. Li, M. Lu, G. Madigan, R. Mccarthy, D.M. Morse, V. Nguyen, T. Orimoto, A. Parker, L. Skinnari, D. Wood

Northwestern University, Evanston, Illinois, U.S.A.
J. Bueghly, S. Dittmer, K.A. Hahn, Y. Liu, M. Mcginnis, Y. Miao, D.G. Monk, M.H. Schmitt, A. Taliercio, M. Velasco

JHEP04(2025)109

University of Notre Dame, Notre Dame, Indiana, U.S.A.
G. Agarwal, R. Band, R. Bucci, S. Castells, A. Das, R. Goldouzian, M. Hildreth, K.W. Ho, K. Hurtado Anampa, T. Ivanov, C. Jessop, K. Lannon, J. Lawrence, N. Loukas, L. Lutton, J. Mariano, N. Marinelli, I. Mcalister, T. McCauley, C. Mcgrady, C. Moore, Y. Musienko[14], H. Nelson, M. Osherson, A. Piccinelli, R. Ruchti, A. Townsend, Y. Wan, M. Wayne, H. Yockey, M. Zarucki, L. Zygala

The Ohio State University, Columbus, Ohio, U.S.A.
A. Basnet, M. Carrigan, L.S. Durkin, C. Hill, M. Joyce, M. Nunez Ornelas, K. Wei, D.A. Wenzl, B.L. Winer, B. R. Yates

Princeton University, Princeton, New Jersey, U.S.A.
H. Bouchamaoui, K. Coldham, P. Das, G. Dezoort, P. Elmer, A. Frankenthal, B. Greenberg, N. Haubrich, K. Kennedy, G. Kopp, S. Kwan, D. Lange, A. Loeliger, D. Marlow, I. Ojalvo, J. Olsen, D. Stickland, C. Tully, L.H. Vage

University of Puerto Rico, Mayaguez, Puerto Rico, U.S.A.
S. Malik, R. Sharma

Purdue University, West Lafayette, Indiana, U.S.A.
A.S. Bakshi, S. Chandra, R. Chawla, A. Gu, L. Gutay, M. Jones, A.W. Jung, A.M. Koshy, M. Liu, G. Negro, N. Neumeister, G. Paspalaki, S. Piperov, V. Scheurer, J.F. Schulte, M. Stojanovic, J. Thieman, A. K. Virdi, F. Wang, A. Wildridge, W. Xie, Y. Yao

Purdue University Northwest, Hammond, Indiana, U.S.A.
J. Dolen, N. Parashar, A. Pathak

Rice University, Houston, Texas, U.S.A.
D. Acosta, T. Carnahan, K.M. Ecklund, P.J. Fernández Manteca, S. Freed, P. Gardner, F.J.M. Geurts, I. Krommydas, W. Li, J. Lin, O. Miguel Colin, B.P. Padley, R. Redjimi, J. Rotter, E. Yigitbasi, Y. Zhang

University of Rochester, Rochester, New York, U.S.A.
A. Bodek, P. de Barbaro, R. Demina, J.L. Dulemba, A. Garcia-Bellido, O. Hindrichs, A. Khukhunaishvili, N. Parmar, P. Parygin[88], R. Taus

Rutgers, The State University of New Jersey, Piscataway, New Jersey, U.S.A.
B. Chiarito, J.P. Chou, S.V. Clark, D. Gadkari, Y. Gershtein, E. Halkiadakis, M. Heindl, C. Houghton, D. Jaroslawski, S. Konstantinou, I. Laflotte, A. Lath, R. Montalvo, K. Nash, J. Reichert, H. Routray, P. Saha, S. Salur, S. Schnetzer, S. Somalwar, R. Stone, S.A. Thayil, S. Thomas, J. Vora, H. Wang

University of Tennessee, Knoxville, Tennessee, U.S.A.
D. Ally, A.G. Delannoy, S. Fiorendi, S. Higginbotham, T. Holmes, A.R. Kanuganti, N. Karunarathna, L. Lee, E. Nibigira, S. Spanier

JHEP04(2025)109

Texas A&M University, College Station, Texas, U.S.A.
D. Aebi, M. Ahmad, T. Akhter, K. Androsov[56], O. Bouhali[89], R. Eusebi, J. Gilmore, T. Huang, T. Kamon[90], H. Kim, S. Luo, R. Mueller, D. Overton, D. Rathjens, A. Safonov

Texas Tech University, Lubbock, Texas, U.S.A.
N. Akchurin, J. Damgov, N. Gogate, V. Hegde, A. Hussain, Y. Kazhykarim, K. Lamichhane, S.W. Lee, A. Mankel, T. Peltola, I. Volobouev

Vanderbilt University, Nashville, Tennessee, U.S.A.
E. Appelt, Y. Chen, S. Greene, A. Gurrola, W. Johns, R. Kunnawalkam Elayavalli, A. Melo, F. Romeo, P. Sheldon, S. Tuo, J. Velkovska, J. Viinikainen

University of Virginia, Charlottesville, Virginia, U.S.A.
B. Cardwell, H. Chung, B. Cox, J. Hakala, R. Hirosky, A. Ledovskoy, C. Neu

Wayne State University, Detroit, Michigan, U.S.A.
S. Bhattacharya, P.E. Karchin

University of Wisconsin — Madison, Madison, Wisconsin, U.S.A.
A. Aravind, S. Banerjee, K. Black, T. Bose, E. Chavez, S. Dasu, P. Everaerts, C. Galloni, H. He, M. Herndon, A. Herve, C.K. Koraka, A. Lanaro, R. Loveless, J. Madhusudanan Sreekala, A. Mallampalli, A. Mohammadi, S. Mondal, G. Parida, L. Pétré, D. Pinna, A. Savin, V. Shang, V. Sharma, W.H. Smith, D. Teague, H.F. Tsoi, W. Vetens, A. Warden

Authors affiliated with an institute or an international laboratory covered by a cooperation agreement with CERN
S. Afanasiev, V. Alexakhin, D. Budkouski, I. Golutvin[†], I. Gorbunov, V. Karjavine, V. Korenkov, A. Lanev, A. Malakhov, V. Matveev[91], V. Palichik, V. Perelygin, M. Savina, V. Shalaev, S. Shmatov, S. Shulha, V. Smirnov, O. Teryaev, N. Voytishin, B.S. Yuldashev[92], A. Zarubin, I. Zhizhin, G. Gavrilov, V. Golovtcov, Y. Ivanov, V. Kim[91], P. Levchenko[93], V. Murzin, V. Oreshkin, D. Sosnov, V. Sulimov, L. Uvarov, A. Vorobyev[†], Yu. Andreev, A. Dermenev, S. Gninenko, N. Golubev, A. Karneyeu, D. Kirpichnikov, M. Kirsanov, N. Krasnikov, I. Tlisova, A. Toropin, T. Aushev, K. Ivanov, V. Gavrilov, N. Lychkovskaya, A. Nikitenko[94,95], V. Popov, A. Zhokin, M. Chadeeva[91], R. Chistov[91], S. Polikarpov[91], V. Andreev, M. Azarkin, M. Kirakosyan, A. Terkulov, E. Boos, V. Bunichev, M. Dubinin[80], L. Dudko, A. Ershov, V. Klyukhin, O. Kodolova[95], S. Obraztsov, M. Perfilov, S. Petrushanko, V. Savrin, G. Vorotnikov, V. Blinov[91], T. Dimova[91], A. Kozyrev[91], O. Radchenko[91], Y. Skovpen[91], V. Kachanov, D. Konstantinov, S. Slabospitskii, A. Uzunian, A. Babaev, V. Borshch, D. Druzhkin[96]

[†] *Deceased*
[1] *Also at Yerevan State University, Yerevan, Armenia*
[2] *Also at TU Wien, Vienna, Austria*
[3] *Also at Ghent University, Ghent, Belgium*

JHEP04(2025)109

[4] *Also at Universidade do Estado do Rio de Janeiro, Rio de Janeiro, Brazil*
[5] *Also at Universidade Estadual de Campinas, Campinas, Brazil*
[6] *Also at Federal University of Rio Grande do Sul, Porto Alegre, Brazil*
[7] *Also at University of Chinese Academy of Sciences, Beijing, China*
[8] *Also at China Center of Advanced Science and Technology, Beijing, China*
[9] *Also at University of Chinese Academy of Sciences, Beijing, China*
[10] *Also at China Spallation Neutron Source, Guangdong, China*
[11] *Now at Henan Normal University, Xinxiang, China*
[12] *Also at University of Shanghai for Science and Technology, Shanghai, China*
[13] *Now at The University of Iowa, Iowa City, Iowa, U.S.A.*
[14] *Also at an institute or an international laboratory covered by a cooperation agreement with CERN*
[15] *Also at Suez University, Suez, Egypt*
[16] *Now at British University in Egypt, Cairo, Egypt*
[17] *Also at Purdue University, West Lafayette, Indiana, U.S.A.*
[18] *Also at Université de Haute Alsace, Mulhouse, France*
[19] *Also at Istinye University, Istanbul, Turkey*
[20] *Also at The University of the State of Amazonas, Manaus, Brazil*
[21] *Also at University of Hamburg, Hamburg, Germany*
[22] *Also at RWTH Aachen University, III. Physikalisches Institut A, Aachen, Germany*
[23] *Also at Bergische University Wuppertal (BUW), Wuppertal, Germany*
[24] *Also at Brandenburg University of Technology, Cottbus, Germany*
[25] *Also at Forschungszentrum Jülich, Juelich, Germany*
[26] *Also at CERN, European Organization for Nuclear Research, Geneva, Switzerland*
[27] *Also at HUN-REN ATOMKI — Institute of Nuclear Research, Debrecen, Hungary*
[28] *Now at Universitatea Babes-Bolyai — Facultatea de Fizica, Cluj-Napoca, Romania*
[29] *Also at MTA-ELTE Lendület CMS Particle and Nuclear Physics Group, Eötvös Loránd University, Budapest, Hungary*
[30] *Also at HUN-REN Wigner Research Centre for Physics, Budapest, Hungary*
[31] *Also at Physics Department, Faculty of Science, Assiut University, Assiut, Egypt*
[32] *Also at Punjab Agricultural University, Ludhiana, India*
[33] *Also at University of Visva-Bharati, Santiniketan, India*
[34] *Also at Indian Institute of Science (IISc), Bangalore, India*
[35] *Also at Amity University Uttar Pradesh, Noida, India*
[36] *Also at IIT Bhubaneswar, Bhubaneswar, India*
[37] *Also at Institute of Physics, Bhubaneswar, India*
[38] *Also at University of Hyderabad, Hyderabad, India*
[39] *Also at Deutsches Elektronen-Synchrotron, Hamburg, Germany*
[40] *Also at Isfahan University of Technology, Isfahan, Iran*
[41] *Also at Sharif University of Technology, Tehran, Iran*
[42] *Also at Department of Physics, University of Science and Technology of Mazandaran, Behshahr, Iran*
[43] *Also at Department of Physics, Faculty of Science, Arak University, ARAK, Iran*
[44] *Also at Helwan University, Cairo, Egypt*
[45] *Also at Italian National Agency for New Technologies, Energy and Sustainable Economic Development, Bologna, Italy*
[46] *Also at Centro Siciliano di Fisica Nucleare e di Struttura Della Materia, Catania, Italy*
[47] *Also at Università degli Studi Guglielmo Marconi, Roma, Italy*
[48] *Also at Scuola Superiore Meridionale, Università di Napoli 'Federico II', Napoli, Italy*
[49] *Also at Fermi National Accelerator Laboratory, Batavia, Illinois, U.S.A.*
[50] *Also at Consiglio Nazionale delle Ricerche — Istituto Officina dei Materiali, Perugia, Italy*
[51] *Also at Department of Applied Physics, Faculty of Science and Technology, Universiti Kebangsaan Malaysia, Bangi, Malaysia*
[52] *Also at Consejo Nacional de Ciencia y Tecnología, Mexico City, Mexico*
[53] *Also at Trincomalee Campus, Eastern University, Sri Lanka, Nilaveli, Sri Lanka*

JHEP04(2025)109

[54] *Also at Saegis Campus, Nugegoda, Sri Lanka*
[55] *Also at National and Kapodistrian University of Athens, Athens, Greece*
[56] *Also at Ecole Polytechnique Fédérale Lausanne, Lausanne, Switzerland*
[57] *Also at University of Vienna, Vienna, Austria*
[58] *Also at Universität Zürich, Zurich, Switzerland*
[59] *Also at Stefan Meyer Institute for Subatomic Physics, Vienna, Austria*
[60] *Also at Laboratoire d'Annecy-le-Vieux de Physique des Particules, IN2P3-CNRS, Annecy-le-Vieux, France*
[61] *Also at Near East University, Research Center of Experimental Health Science, Mersin, Turkey*
[62] *Also at Konya Technical University, Konya, Turkey*
[63] *Also at Izmir Bakircay University, Izmir, Turkey*
[64] *Also at Adiyaman University, Adiyaman, Turkey*
[65] *Also at Bozok Universitetesi Rektörlügü, Yozgat, Turkey*
[66] *Also at Marmara University, Istanbul, Turkey*
[67] *Also at Milli Savunma University, Istanbul, Turkey*
[68] *Also at Kafkas University, Kars, Turkey*
[69] *Now at Istanbul Okan University, Istanbul, Turkey*
[70] *Also at Hacettepe University, Ankara, Turkey*
[71] *Also at Erzincan Binali Yildirim University, Erzincan, Turkey*
[72] *Also at Istanbul University — Cerrahpasa, Faculty of Engineering, Istanbul, Turkey*
[73] *Also at Yildiz Technical University, Istanbul, Turkey*
[74] *Also at School of Physics and Astronomy, University of Southampton, Southampton, United Kingdom*
[75] *Also at IPPP Durham University, Durham, United Kingdom*
[76] *Also at Monash University, Faculty of Science, Clayton, Australia*
[77] *Also at Università di Torino, Torino, Italy*
[78] *Also at Bethel University, St. Paul, Minnesota, U.S.A.*
[79] *Also at Karamanoğlu Mehmetbey University, Karaman, Turkey*
[80] *Also at California Institute of Technology, Pasadena, California, U.S.A.*
[81] *Also at United States Naval Academy, Annapolis, Maryland, U.S.A.*
[82] *Also at Ain Shams University, Cairo, Egypt*
[83] *Also at Bingol University, Bingol, Turkey*
[84] *Also at Georgian Technical University, Tbilisi, Georgia*
[85] *Also at Sinop University, Sinop, Turkey*
[86] *Also at Erciyes University, Kayseri, Turkey*
[87] *Also at Horia Hulubei National Institute of Physics and Nuclear Engineering (IFIN-HH), Bucharest, Romania*
[88] *Now at another institute or international laboratory covered by a cooperation agreement with CERN*
[89] *Also at Texas A&M University at Qatar, Doha, Qatar*
[90] *Also at Kyungpook National University, Daegu, Korea*
[91] *Also at another institute or international laboratory covered by a cooperation agreement with CERN*
[92] *Also at Institute of Nuclear Physics of the Uzbekistan Academy of Sciences, Tashkent, Uzbekistan*
[93] *Also at Northeastern University, Boston, Massachusetts, U.S.A.*
[94] *Also at Imperial College, London, United Kingdom*
[95] *Now at Yerevan Physics Institute, Yerevan, Armenia*
[96] *Also at Universiteit Antwerpen, Antwerpen, Belgium*

JHEP04(2025)109